

Sequential learning and control: Targeted exploration for robust performance

Janani Venkatasubramanian¹, Johannes Köhler², Julian Berberich¹, Frank Allgöwer¹

Abstract—We present a novel dual control strategy for uncertain linear systems based on targeted harmonic exploration and gain-scheduling with performance and excitation guarantees. In the proposed sequential approach, robust control is implemented after exploration with the main feature that the exploration is optimized with respect to the robust control performance. Specifically, we leverage recent results on finite excitation using spectral lines to determine a high probability lower bound on the resultant finite excitation of the exploration data. This provides an a priori upper bound on the remaining model uncertainty after exploration, which can further be leveraged in a gain-scheduling controller design that guarantees robust performance. This leads to a semidefinite program-based design which computes an exploration strategy with finite excitation bounds and minimal energy, and a gain-scheduled controller with probabilistic performance bounds that can be implemented after exploration. The effectiveness of our approach and its benefits over common random exploration strategies are demonstrated with an example of a system which is ‘hard to learn’.

Index Terms—Identification for control, Dual control, Robust control, Uncertain systems

I. INTRODUCTION

Control inputs to an uncertain system should have a ‘directing effect’ to control the dynamical system and achieve a certain goal. Furthermore, the inputs should also have a ‘probing’ effect to learn the uncertainty in the system. These two effects are, however, competing and draw attention to the exploration - exploitation trade-off, which is also the subject of contemporary literature on Reinforcement Learning [1]. In close association with these effects, simultaneous learning and control of uncertain dynamic systems has garnered research interest with the establishment of the *dual control* paradigm [2]. A detailed survey of dual control methods is provided in [3], [4]. These methods laid the foundation of balancing exploration with caution.

Early works in this direction involve approximations of stochastic Dynamic Programming (DP), known as implicit dual control methods, to handle computational intractability

problems that accompany stochastic DP [5]–[8]. Another class of dual control, known as explicit dual control methods, use heuristic probing techniques to actively learn the uncertain system [9], and are closely related to *Optimal Experiment Design* [10], [11]. These methods solve the combined problem of regulating and probing closed-loop system dynamics, and have been further refined to explicitly consider the relevance of the uncertainty in the cost function, yielding application-oriented strategies [12]–[14].

A particularly appealing approach to the dual control problem is to sequentially apply some probing input for exploration, and then design a robustly stabilizing feedback based on the gathered data. Recent methods focus on *targeted* exploration, and perform better than methods that use common greedy random exploration [15]–[20]. In particular, these methods consider that exploration should be targeted in the sense that the resulting uncertainty reduction in the model facilitates achieving a control goal and performance objective. Identification strategies with possibly small experiment cost are proposed in [15]–[17], however only with asymptotic excitation guarantees. In [15], identification and robust control are jointly designed, and the designed identification is asymptotic. Consequently, iterations of identification and robust control design are employed to ensure the uncertain parameters meet a desired accuracy that is required for robust control. Hence, in [15], guarantees for finite data experiment and identification are not derived, and identification does not directly yield the desired properties for robust control. Unlike [15]–[17], the approaches in [18]–[21] focus on non-asymptotic targeted exploration and approximate a desired uncertainty bound over a finite duration of identification.

A targeted exploration strategy that excites the system to reduce uncertainty specifically to improve a robust LQR design is introduced in [18]. This approach relies on a high probability uncertainty bound on system parameters which can be approximately predicted and thus optimized depending on the exploration input. Developing on the works in [18] and [15], a dual control strategy is proposed in [19] that minimizes the worst-case cost achieved by a robust controller that is synthesized with reduced model uncertainty. The approach in [20] extends the exploration strategy in [18] to a more realistic finite horizon problem setting that captures the trade-offs between exploration and exploitation better.

The exploration methods proposed in [18]–[20] use a linear state-feedback and an additional Gaussian noise term for exploration. To tractably compute the predicted uncertainty bound associated with the parameter estimates after exploration, the empirical covariance is approximated by the worst-

¹ Janani Venkatasubramanian, Julian Berberich and Frank Allgöwer are with the Institute for Systems Theory and Automatic Control, University of Stuttgart, 70550 Stuttgart, Germany. (email:{janani.venkatasubramanian, julian.berberich, frank.allgower}@ist.uni-stuttgart.de)

² Johannes Köhler is with the Institute for Dynamic Systems and Control, ETH Zürich, Zürich CH-80092, Switzerland. (email:jkoehle@ethz.ch)

F. Allgöwer is thankful that his work was funded by Deutsche Forschungsgemeinschaft (DFG, German Research Foundation) under Germany’s Excellence Strategy - EXC 2075 - 390740016 and under grant 468094890. F. Allgöwer acknowledges the support by the Stuttgart Center for Simulation Science (SimTech). Janani Venkatasubramanian thanks the International Max Planck Research School for Intelligent Systems (IMPRS-IS) for supporting her.

case state covariance. This approximation fails to provide a priori guarantees of excitation on the exploration inputs. While the results of methods in [15], [18]–[20] seem to perform well numerically, they lack the corresponding theoretical performance guarantees. In particular, changes in the mean of uncertain system parameters during the exploration phase are not accounted for in the methods in [18], [19]. We address these limitations with guaranteed (non-asymptotic) finite excitation in combination with our recently proposed gain-scheduled controller [21], which accounts for changing parameter estimates and guarantees closed-loop performance.

In particular, we propose harmonic exploration inputs in the form of a linear combination of sinusoids of specific frequencies and optimized amplitudes, and reduce uncertainty in a targeted fashion with the goal of guaranteed control performance. This choice is also supported in literature, where it was established that the robust optimal control input can be expressed with appropriately chosen amplitudes and frequencies of the sinusoids [22]. As one of our main contributions, we derive an *a priori* guaranteed lower bound on the finite excitation of the exploration inputs depending on the spectral content of the inputs [23]. The lower bound on excitation results in a bound on the uncertain system parameters, which can be leveraged in robust control design to provide performance guarantees. Regarding the application of targeted exploration in dual control, we employ the exploration strategy in our recently proposed gain-scheduling-based dual control approach [21]. In particular, we treat the mean of future uncertain system parameters as a scheduling variable. The approach based on gain-scheduling gives rise to a design based on a semidefinite program (SDP) with closed-loop performance guarantees under reasonable assumptions. The resulting controller is a state feedback which depends on the parameter estimates after the exploration phase and thus, on the data collected during this phase. The controller *guarantees* robust closed-loop performance after an initial exploration phase.

II. PROBLEM STATEMENT

Notation: The transpose of a matrix $A \in \mathbb{R}^{n \times m}$ is denoted by A^\top . The conjugate transpose of a matrix $A \in \mathbb{C}^{n \times m}$ is denoted by A^H . The positive definiteness of a matrix $A \in \mathbb{C}^{n \times m}$ is denoted by $A = A^H \succ 0$. The Kronecker product operator is denoted by \otimes . The operator $\text{vec}(A)$ stacks the columns of A to form a vector. The operator $\text{diag}(A_1, \dots, A_n)$ creates a block diagonal matrix by aligning the matrices A_1, \dots, A_n along the diagonal starting with A_1 in the upper left corner. The critical value of the Chi-squared distribution with n degrees of freedom and probability p is denoted by $\chi_n^2(p)$. A unit sphere of dimension d is denoted by \mathcal{S}^{d-1} . The expected value of a random variable X is denoted by $\mathbb{E}(X)$. The probability of an event E occurring is denoted by $\mathbb{P}(E)$. Given a sequence $\{x_k\}_{k=0}^{T-1}$, the discrete Fourier transform (DFT) of the sequence is denoted by $\mathbf{x}(e^{j\omega}) = \sum_{k=0}^{T-1} x_k e^{-j2\pi k\omega}$ where $\omega \in \Omega_T := \{0, 1/T, \dots, (T-1)/T\}$. For a vector $x \in \mathbb{R}^n$ and a matrix $P \succ 0$, the Euclidean norm is denoted by $\|x\| = \sqrt{x^\top x}$ and $\|x\|_P = \sqrt{x^\top P x}$. For a matrix $A \in \mathbb{C}^{m \times n}$,

$\|A\|$ denotes the largest singular value. Furthermore, given a matrix $M \succeq 0$, $\|A\|_M = \|M^{1/2}A\|$. A random variable $X \in \mathbb{R}^d$ that is normally distributed with mean μ and variance Σ is denoted by $X \sim \mathcal{N}(\mu, \Sigma)$.

A random variable $X \in \mathbb{R}$ is said to be sub-Gaussian [24], with variance proxy $\sigma^2 \in \mathbb{R}$, i.e., $X \sim \text{subG}(\sigma^2)$, if $\mathbb{E}(X) = 0$ and its moment generating function satisfies

$$\mathbb{E}(e^{sX}) \leq e^{\left(\frac{\sigma^2 s^2}{2}\right)}, \quad \forall s \in \mathbb{R}. \quad (1)$$

A random vector $X \in \mathbb{R}^d$ is said to be sub-Gaussian with variance proxy σ^2 , i.e., $X \sim \text{subG}(\sigma^2)$, if $\mathbb{E}[X] = 0$ and $u^\top X$ is sub-Gaussian with variance proxy σ^2 for any unit vector $u \in \mathcal{S}^{d-1}$.

A. Setting

Consider a discrete-time linear time-invariant dynamical system of the form

$$x_{k+1} = A_{\text{tr}}x_k + B_{\text{tr}}u_k + w_k, \quad w_k \stackrel{\text{i.i.d.}}{\sim} \mathcal{N}(0, \sigma_w^2 I_{n_x}) \quad (2)$$

where $x_k \in \mathbb{R}^{n_x}$ is the state, $u_k \in \mathbb{R}^{n_u}$ is the control input, and $w_k \in \mathbb{R}^{n_x}$ is the normally distributed process noise. It is assumed that the realizations of w_k are independent and identically distributed (i.i.d.) with zero mean and known variance $\sigma_w^2 I_{n_x}$, and the state x_k is directly measurable. These assumptions allow for the application of standard identification results. The true values of the system parameters $A_{\text{tr}}, B_{\text{tr}}$, are initially uncertain, and there is a need to gather informative data to improve the accuracy of the parameters.

Control goal: The overarching goal of the proposed dual control strategy is to design a stabilizing state-feedback controller $u_k = Kx_k$ which ensures that the closed-loop system is stable while also satisfying some desired performance specifications with high probability [25], [26]. Consider the output $z_k \in \mathbb{R}^{n_z}$ that depends on the state and control input:

$$z_k = Cx_k + D_u u_k, \quad (3)$$

where C and D_u are known. Note that z_k is the closed-loop trajectory resulting from the application of the input $u_k = Kx_k$. In the presence of white noise input signals, the H_2 -norm provides a suitable stochastic interpretation in terms of the asymptotic output variance of the closed-loop system. H_2 performance is specified in terms of the H_2 -norm of the closed-loop system given by $\lim_{k \rightarrow \infty} \mathbb{E}(\|z_k\|_2)^2$ for white noise inputs $w_k \sim \mathcal{N}(0, \sigma_w^2 I_{n_x})$ [27].

Definition 1. (*H_2 performance*) The closed-loop system with $u_k = Kx_k$ achieves the H_2 performance bound γ_p if

$$\lim_{k \rightarrow \infty} \mathbb{E}(\|z_k\|_2)^2 < \gamma_p^2 \quad (4)$$

for $w_k \sim \mathcal{N}(0, \sigma_w^2 I_{n_x})$ and the initial state $x_0 = 0$.

Due to the uncertain dynamics, we cannot directly design a linear feedback $u_k = Kx_k$ that systematically accounts for the change in the mean estimate after exploration and achieves a desired H_2 performance bound γ_p (Def. 1). Instead, we propose a sequential dual control approach wherein a targeted exploration strategy is implemented first, which is followed by

the implementation of a parametrized state-feedback achieving (4). To this end, we first provide preliminaries regarding uncertainty bounds for parameter estimation based on time-series data and spectral information in Section III. As one of the main results, we derive the exploration strategy, and the corresponding uncertainty bound on the data obtained during exploration in Section IV. The primary challenge is to encapsulate the dual effect of the performance improvement through the process of exploration, and to tailor the exploration in a manner that is pertinent to performance improvement. Therefore, we simultaneously design the targeted exploration strategy and a parametrized state-feedback controller for the system in (2) in dependence of the future parameters/model estimate. The new parameter estimate, which influences the state-feedback control law K , is interpreted as a scheduling variable using tools from gain-scheduling control [21]. The gain-scheduling controller is presented in Section V. Consequently, we solve a joint dual control problem of obtaining the exploration strategy and the state-feedback controller to be implemented after exploration without re-design, as elaborated in Section VI. A sketch of the overall dual control strategy is provided in Fig. 1. The design process ensures that, by applying the feedback after the phase of exploration, H_2 performance specifications are guaranteed with high probability.

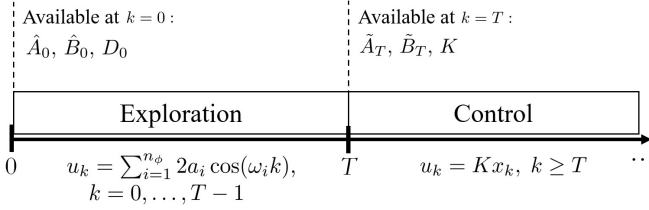


Fig. 1: Sketch of the sequential robust dual control strategy.

III. PRELIMINARIES

This section discusses prior results that provide a data-dependent uncertainty bound on the parameter estimates, and the required preliminaries regarding the theory of spectral lines, from [18] and [23], respectively.

A. Uncertainty bound

Given observed data $\mathcal{D}_T = \{x_k, u_k\}_{k=0}^{T-1}$ of length T , we are interested in quantifying the uncertainty associated with unknown parameters A_{tr} and B_{tr} . Henceforth, we denote $\phi_k = [x_k^\top \ u_k^\top]^\top \in \mathbb{R}^{n_\phi}$ where $n_\phi = n_x + n_u$. In our setting, we assume that some prior knowledge on the dynamics is available.

Assumption 1. *The parameters $\theta = \text{vec}(A, B)$ have a Gaussian prior, i.e., $\theta \sim \mathcal{N}(\hat{\theta}_{\text{prior}}, \Sigma_{\theta, \text{prior}})$. Furthermore, there exists a matrix $\tilde{D}_0 \succ 0$ such that $\Sigma_{\theta, \text{prior}}^{-1} = \tilde{D}_0 \otimes I_{n_x}$.*

The estimate $\hat{\theta}_T = \text{vec}([\hat{A}_T, \hat{B}_T])$ is the maximum a posteriori (MAP) estimate of the unknown parameters A_{tr} and B_{tr} , and is computed as:

$$\hat{\theta}_T = \arg \min_{\theta} \sum_{k=0}^{T-1} \frac{1}{\sigma_w^2} \left\| (x_{k+1} - ([x_k^\top \ u_k^\top] \otimes I_{n_x}) \theta) \right\|^2 + \left\| \theta - \hat{\theta}_{\text{prior}} \right\|_{\Sigma_{\theta, \text{prior}}^{-1}}^2 \quad (5)$$

with posterior covariance

$$\Sigma_{\theta, \text{post}}^{-1} = \Sigma_{\theta, \text{prior}}^{-1} + \left(\frac{1}{\sigma_w^2} \sum_{k=0}^{T-1} \phi_k \phi_k^\top \right) \otimes I_{n_x}. \quad (6)$$

Under Assumption 1, the posterior distribution $p(\theta|\mathcal{D})$ is given by $\mathcal{N}(\hat{\theta}_T, \Sigma_{\theta, \text{post}})$ [18, Prop. 2.1].

Remark 1. *In case a prior as in Assumption 1 is not available, it can also be inferred from data. More precisely, given a data set $\mathcal{D}_0 = \{\phi_k\}_{k=-\tilde{T}}^{-1}$ obtained from a randomly exciting input, and a uniform prior over the parameters $\theta = \text{vec}([A, B])$, i.e., $p(\theta) \propto 1$, the posterior distribution is given by $\mathcal{N}(\hat{\theta}, \Sigma_\theta)$, where $\hat{\theta} = \text{vec}([\hat{A}, \hat{B}])$ is the ordinary least squares estimate, and $\Sigma_\theta^{-1} = \left(\frac{1}{\sigma_w^2} \sum_{k=-\tilde{T}}^{-1} \phi_k \phi_k^\top \right) \otimes I_{n_x} = \tilde{D}_0 \otimes I_{n_x}$. This also justifies the structural assumption on $\Sigma_{\theta, \text{prior}}^{-1}$ being of the form $\tilde{D}_0 \otimes I_{n_x}$ for some $\tilde{D}_0 \succ 0$.*

The following lemma provides high-probability credibility regions for the uncertain parameters θ , and the uncertain system matrices A, B .

Lemma 1. [18, Prop. 2.1, Lem. 3.1] *Let Assumption 1 hold. Given data set \mathcal{D}_T of length T with estimate $\hat{\theta}_T = \text{vec}([\hat{A}_T, \hat{B}_T])$ (cf. (5)), set $D_T = \frac{1}{c_\delta \sigma_w^2} \sum_{k=0}^{T-1} \phi_k \phi_k^\top$, $D_0 = \frac{1}{c_\delta} \tilde{D}_0$, $c_\delta = \chi_{n_x n_\phi}^2(\delta)$ with $0 < \delta < 1$. Then,*

I. $\mathbb{P}(\theta_{\text{tr}} = \text{vec}([A_{\text{tr}}, B_{\text{tr}}]) \in \Theta) \geq 1 - \delta$, where

$$\Theta := \left\{ \theta : (\theta - \hat{\theta}_T)^\top \Sigma_{\theta, \text{post}}^{-1} (\theta - \hat{\theta}_T) \leq c_\delta \right\} \quad (7)$$

with $\Sigma_{\theta, \text{post}}^{-1} = \Sigma_{\theta, \text{prior}}^{-1} + (c_\delta D_T) \otimes I_{n_x}$, and

II. $\mathbb{P}([A_{\text{tr}}, B_{\text{tr}}] \in \Delta) \geq 1 - \delta$, where

$$\Delta := \left\{ A, B : \begin{bmatrix} (\hat{A}_T - A)^\top \\ (\hat{B}_T - B)^\top \end{bmatrix}^\top D_{\text{post}} \begin{bmatrix} (\hat{A}_T - A)^\top \\ (\hat{B}_T - B)^\top \end{bmatrix} \preceq I \right\} \quad (8)$$

with $D_{\text{post}} = D_0 + D_T$.

The result of Lemma 1 is a data-dependent uncertainty bound that can be utilized to synthesize robust controllers similar to approaches in [18]–[21]. Note that statement **I** implies statement **II** of Lemma 1 [18]. In Section IV, we use this result to derive a suitable targeted exploration strategy.

Initial estimates of the system parameters can be obtained from the mean of the prior distribution via $\text{vec}([\hat{A}_0, \hat{B}_0]) = \hat{\theta}_{\text{prior}}$. The matrix D_0 quantifies the robust bound associated with these initial estimates for a given probability $1 - \delta$. More precisely, from Lemma 1, $\theta_{\text{tr}} \in \Theta_0$ with probability at least $1 - \delta$, where

$$\Theta_0 := \left\{ \theta : (\hat{\theta}_{\text{prior}} - \theta)^\top (D_0 \otimes I_{n_x}) (\hat{\theta}_{\text{prior}} - \theta) \leq 1 \right\}, \quad (9)$$

and $[A_{\text{tr}}, B_{\text{tr}}] \in \Delta_0$ with probability at least $1 - \delta$ where

$$\Delta_0 := \left\{ A, B : \begin{bmatrix} (\hat{A}_0 - A)^\top \\ (\hat{B}_0 - B)^\top \end{bmatrix}^\top D_0 \begin{bmatrix} (\hat{A}_0 - A)^\top \\ (\hat{B}_0 - B)^\top \end{bmatrix} \preceq I \right\}. \quad (10)$$

Denote

$$\Delta_0 = [A_{\text{tr}} - \hat{A}_0 \quad B_{\text{tr}} - \hat{B}_0]. \quad (11)$$

By applying the Schur complement twice on (10), Lemma 1 implies that

$$\mathbb{P}(\Delta_0^\top \Delta_0 \preceq D_0^{-1}) \geq 1 - \delta. \quad (12)$$

Through the targeted exploration process for T time steps as elaborated in Section IV, data $\mathcal{D}_T = \{\phi_k\}_{k=0}^{T-1}$ will be observed. The new estimates \hat{A}_T and \hat{B}_T will be computed from data \mathcal{D}_T and the prior information as in (5), and made available at time T . The matrix $D_{\text{post}} := D_0 + \frac{1}{c_s \sigma_w^2} \sum_{k=0}^{T-1} \phi_k \phi_k^\top$ quantifies the uncertainty associated with the estimates \hat{A}_T and \hat{B}_T (cf. Lemma 1).

B. Frequency domain information using spectral lines

This subsection discusses preliminaries for finite excitation based on the theory of spectral lines, which deals with the analysis of frequency domain information that can be derived from time-series data [23]. The finite-data uncertainty bounds in Lemma 1 are based on the matrix D_T , which is a quantitative measure of finite excitation [23, Def. 3]. The following notion of a sub-Gaussian spectral line is introduced.

Definition 2. (Sub-Gaussian Spectral Line [23]) *A stochastic sequence $\{\phi_k\}_{k=0}^{T-1}$ is said to have a sub-Gaussian spectral line from $k = 0$ to $T - 1$ at a frequency $\omega_0 \in \Omega_T$ with amplitude $\bar{\phi}(\omega_0) \in \mathbb{C}^{n_\phi}$ and a radius $R > 0$ if*

$$\frac{1}{T} \sum_{k=0}^{T-1} \phi_k e^{-j2\pi\omega_0 k} - \bar{\phi}(\omega_0) \sim \text{subG}(R^2/T). \quad (13)$$

If noise is neglected, we recover a deterministic frequency component

$$\bar{\phi}(\omega_0) = \frac{1}{T} \sum_{k=0}^{T-1} \phi_k e^{-j2\pi\omega_0 k}. \quad (14)$$

The radius R in Definition 2 is a measure of the stochastic process noise. The notion of a sub-Gaussian spectral line induces a requirement of appropriate behaviour over finite time. If the input has sufficiently many spectral lines, then the input signal is finitely exciting and can be used to provide bounds for parameter estimation.

In order to establish the relationship between the spectral content of the input signal and finite excitation, the expected information matrix is first defined as follows.

Definition 3. (Expected Information Matrix [23]) *Given a sequence $\{\phi_k\}_{k=0}^{T-1}$ with L sub-Gaussian spectral lines at frequencies $\omega_i \in \Omega_T$, $i = 1, \dots, L$ with amplitudes $\{\bar{\phi}(\omega_i)\}_{i=1}^L$, the information matrix $\bar{\Phi} \in \mathbb{C}^{n_\phi \times L}$ is defined as*

$$\bar{\Phi} = \begin{bmatrix} | & \dots & | \\ \bar{\phi}(\omega_1) & \dots & \bar{\phi}(\omega_L) \\ | & \dots & | \end{bmatrix}. \quad (15)$$

The spectral content in the expected information matrix can be used to determine whether a signal is finitely exciting or not [23]. In deterministic system identification, estimation of unknown parameters is made possible if $\bar{\Phi}$ has full rank and is numerically well conditioned. Since $\omega_i \in \Omega_T$, $i = 1, \dots, L$, we set $T \geq L$ and select L frequencies from Ω_T .

IV. TARGETED EXPLORATION

In this section, we propose a targeted exploration strategy based on a derived uncertainty bound on the data obtained through the process of exploration. Unlike greedy random exploration [18]–[21], we introduce a targeted exploration strategy in the form of a linear combination of sinusoids with specified frequencies that explicitly shape the model uncertainty. In particular, this is achieved by deriving a lower bound on finite excitation of the exploration data using the spectral information of the exploration inputs in Lemma 2. Since this bound is non-convex in the decision variables and depends on uncertain model parameters, a convex relaxation procedure is carried out (cf. Section IV-C), and required bounds on the effect of the model uncertainty are derived (cf. Section IV-D). Finally, in Section IV-E, we obtain an LMI for exploration which provides us with exploration inputs that guarantee a lower-bound on the finite excitation. In Section VI, the results of this section will be combined with a robust (gain-scheduled) control design to achieve a guaranteed performance after exploration.

A. Exploration strategy

The exploration input sequence takes the form

$$u_k = \sum_{i=1}^L 2a_i \cos(\omega_i k), \quad k = 0, \dots, T-1 \quad (16)$$

where T is the exploration time and $a_i \in \mathbb{R}^{n_u \times 1}$ are the amplitudes of the sinusoidal inputs at L distinctly selected frequencies $\omega_i \in \Omega_T$. Since the input signal is deterministic and sinusoidal, the amplitude of the spectral line is $\bar{u}(\omega_i) = a_i$, and the radius of the spectral line is 0 (cf. Def. 2). Denote $U_e = \text{diag}(a_1, \dots, a_L) \in \mathbb{R}^{L n_u \times L}$. The exploration input is computed such that it excites the system sufficiently with minimal control energy, based on the initial parameter estimates. To this end, we require that the control energy at each time instant does not exceed γ_e^2 , i.e., $\sum_{i=1}^L \|a_i\|^2 = \mathbf{1}_L^\top U_e^\top U_e \mathbf{1}_L \preceq \gamma_e^2$ where $\mathbf{1}_L \in \mathbb{R}^{L \times 1}$ is a vector of ones, and the bound $\gamma_e \geq 0$ is desired to be small. Using the Schur complement, this criterion is equivalent to

$$S_{\text{energy-bound}}(\gamma_e, U_e) := \begin{bmatrix} \gamma_e & \mathbf{1}_L^\top U_e^\top \\ U_e \mathbf{1}_L & \gamma_e I \end{bmatrix} \succeq 0. \quad (17)$$

Since we consider only open-loop inputs in our exploration strategy, we require A_{tr} to be Schur stable.

Remark 2. *An exploration input of the form in (16) with an additional linear feedback, i.e., $v_k = u_k + Kx_k$, which robustly stabilizes the initial estimate and prior uncertainty, may be considered if it is not known whether the system is Schur stable.*

B. Bound on finite excitation

For the system evolving under the exploration input as given in (16), the uncertainty bound on the parameters can be computed from the expected information matrix $\bar{\Phi}$ of the input. As a prerequisite to computing the uncertainty bound, it is necessary to establish the relationship between the spectral content of the observed state x_k and the applied input u_k . At a frequency ω_i , the relation between ϕ_k , u_k and w_k is

$$\begin{aligned} \phi(e^{j\omega_i}) &= \underbrace{\begin{bmatrix} (e^{j\omega_i} I - A_{\text{tr}})^{-1} B_{\text{tr}} \\ I_{n_u} \end{bmatrix}}_{V_i} \mathbf{u}(e^{j\omega_i}) \\ &+ \underbrace{\begin{bmatrix} (e^{j\omega_i} I - A_{\text{tr}})^{-1} \\ 0 \end{bmatrix}}_{Y_i} \mathbf{w}(e^{j\omega_i}). \end{aligned} \quad (18)$$

Given u_k as in (16) and using [23, Lemma 1], ϕ_k has L sub-Gaussian spectral lines (cf. Def. 2) from 0 to $T-1$ at distinct frequencies $\omega_i \in \Omega_T$, $i = 1, \dots, L$ with amplitudes

$$\bar{\phi}(\omega_i) = V_i \bar{u}(\omega_i) \quad (19)$$

and radii $\|Y_i\| \sigma_w$. Denote

$$V_{\text{tr}} = [V_1, \dots, V_L] \in \mathbb{C}^{n_\phi \times L n_u}, \quad (20)$$

which is unknown since the true dynamics A_{tr} , B_{tr} are unknown. Then, the expected information matrix $\bar{\Phi} \in \mathbb{C}^{n_\phi \times L}$ (cf. Def. 3) is

$$\bar{\Phi} = V_{\text{tr}} U_e. \quad (21)$$

Denote

$$\begin{aligned} Y_{\text{tr}} &= [Y_1, \dots, Y_{n_\phi}] \in \mathbb{C}^{n_\phi \times L n_x}, \\ W &= \text{diag}(\mathbf{w}(e^{j\omega_1}), \dots, \mathbf{w}(e^{j\omega_{n_\phi}})) \in \mathbb{C}^{L n_x \times L} \end{aligned} \quad (22)$$

and

$$\tilde{W} = Y_{\text{tr}} W. \quad (23)$$

The effect of the noise w is captured by W . Each block $\mathbf{w}(e^{j\omega_i})$, $i = 1, \dots, L$, on the diagonal of W is Gaussian, i.e., $\mathbf{w}(e^{j\omega_i}) \sim \mathcal{N}(0, \sigma_w^2 I)$ with $\sigma_w^2 = \frac{\sigma_w^2}{T}$, since the DFT of a Gaussian signal is also Gaussian, but with a distinct variance (cf. Appendix D). The following lemma, inspired by [23, Proposition 3]¹, presents a clear relationship between the spectral content of the signal and finite excitation.

Lemma 2. For any $\epsilon \in (0, 1)$, ϕ_k satisfies

$$\frac{1}{T} \sum_{k=0}^{T-1} \phi_k \phi_k^\top \succeq \frac{1}{L} \left((1-\epsilon) \bar{\Phi} \bar{\Phi}^\text{H} + \left(\frac{\epsilon-1}{\epsilon} \right) \tilde{W} \tilde{W}^\text{H} \right). \quad (24)$$

¹The penultimate step in the proof of [23, Prop. 3, Appendix D] results in $\|\bar{\Phi} + \tilde{W}\|^2 \geq \|\bar{\Phi}^{-1}\|^{-2} - \|\tilde{W}\|^2$, which is incorrect, in general. The authors of [23] have prepared a corrigendum [28] that avoids these arguments in the proof of [23, Prop. 3, Appendix D].

Proof. Note that for any unit vector $z \in \mathbb{C}^{n_\phi}$, and any realization $\{\phi_k\}_{k=0}^{T-1}$,

$$\begin{aligned} z^\text{H} \left(\frac{1}{T} \sum_{k=0}^{T-1} \phi_k \phi_k^\top \right) z &= \frac{1}{T} \sum_{k=0}^{T-1} |\phi_k^\top z|^2 \\ &= \frac{1}{T} \sum_{k=0}^{T-1} |\phi_k^\top z|^2 \cdot \underbrace{\frac{1}{L} \sum_{l=1}^L |e^{-j2\pi\omega_l k}|^2}_{=1} \\ &\geq \frac{1}{L} \sum_{l=1}^L \left| \frac{1}{T} \sum_{k=0}^{T-1} \phi_k^\top z e^{-j2\pi\omega_l k} \right|^2, \end{aligned} \quad (25)$$

by Jensen's inequality. This leads to

$$\begin{aligned} z^\text{H} \left(\frac{1}{T} \sum_{k=0}^{T-1} \phi_k \phi_k^\top \right) z &\geq \frac{1}{L} \sum_{l=1}^L \left| \frac{1}{T} \sum_{k=0}^{T-1} \phi_k^\top z e^{-j2\pi\omega_l k} \right|^2 \\ &= \frac{1}{L} \left(z^\text{H} (\bar{\Phi} + \tilde{W}) (\bar{\Phi} + \tilde{W})^\text{H} z \right). \end{aligned} \quad (26)$$

By Young's inequality [29], for any $\epsilon > 0$, we have

$$\bar{\Phi} \tilde{W}^\text{H} + \tilde{W} \bar{\Phi}^\text{H} \succeq -\epsilon \bar{\Phi} \bar{\Phi}^\text{H} - \frac{1}{\epsilon} \tilde{W} \tilde{W}^\text{H} \quad (27)$$

and hence

$$(\bar{\Phi} + \tilde{W})(\bar{\Phi} + \tilde{W})^\text{H} \succeq (1-\epsilon) \bar{\Phi} \bar{\Phi}^\text{H} - \left(\frac{1-\epsilon}{\epsilon} \right) \tilde{W} \tilde{W}^\text{H}. \quad (28)$$

By inserting Inequality (28) in Inequality (26), we get (24). \square

From Lemma 2, using (21) and (24), for any $\epsilon \in (0, 1)$, ϕ_k satisfies

$$\frac{1}{\bar{c}} \underbrace{\sum_{k=0}^{T-1} \phi_k \phi_k^\top}_{D_T} \succeq \frac{T}{\bar{c}L} \left((1-\epsilon) V_{\text{tr}} U_e U_e^\top V_{\text{tr}}^\text{H} - \left(\frac{1-\epsilon}{\epsilon} \right) \tilde{W} \tilde{W}^\text{H} \right) \quad (29)$$

where $\bar{c} = \sigma_w^2 c_\delta$.

Inequality (29) allows us to determine a lower bound on the finite excitation $D_{\text{post}} = D_0 + D_T$, and thus upper-bound the uncertainty of the MAP estimate using Lemma 1. Note that this lower bound depends on the amplitudes of the harmonic signals U_e (cf. (15), (21)), as well as on the size of the noise. However, determining a lower bound on D_T based on Inequality (29) results in non-convex constraints in the decision variable U_e . We circumvent this issue by using a convex relaxation procedure.

C. Convex relaxation

The following lemma provides a lower bound on D_T which is linear in U_e .

Lemma 3. For any matrices $\tilde{U} \in \mathbb{R}^{L n_u \times L}$ and $U_e \in \mathbb{R}^{L n_u \times L}$, and any $\epsilon \in (0, 1)$, we have:

$$\begin{aligned} \frac{\bar{c} n_\phi}{T} D_T &\succeq (1-\epsilon) \left(V_{\text{tr}} \left(U_e \tilde{U}^\top + \tilde{U} U_e^\top - \tilde{U} \tilde{U}^\top \right) V_{\text{tr}}^\text{H} \right) \\ &- \left(\frac{1-\epsilon}{\epsilon} \right) \tilde{W} \tilde{W}^\text{H}. \end{aligned} \quad (30)$$

$$S_{\text{exploration}}(\epsilon, \tau, \tilde{U}, U_e, \hat{V}, l, \bar{D}_T, \Gamma_v) = \begin{bmatrix} (1-\epsilon)(U_e^\top \tilde{U} + \tilde{U}^\top U_e - \tilde{U}^\top \tilde{U}) & 0 \\ 0 & -(\frac{1-\epsilon}{\epsilon})l^2 I - \frac{\bar{c}L}{T}\bar{D}_T \end{bmatrix} - \tau \begin{bmatrix} -I & \hat{V}^\text{H} \\ \hat{V} & \Gamma_v - \hat{V}\hat{V}^\text{H} \end{bmatrix} \succeq 0 \quad (31)$$

Proof. We have

$$\begin{aligned} & V_{\text{tr}} U_e U_e^\top V_{\text{tr}}^\text{H} - V_{\text{tr}} U_e \tilde{U}^\top V_{\text{tr}}^\text{H} - V_{\text{tr}} \tilde{U} U_e^\top V_{\text{tr}}^\text{H} + V_{\text{tr}} \tilde{U} \tilde{U}^\top V_{\text{tr}}^\text{H} \\ &= V_{\text{tr}} (U_e - \tilde{U})(U_e - \tilde{U})^\top V_{\text{tr}}^\text{H} \\ &\succeq 0 \end{aligned}$$

and hence

$$V_{\text{tr}} U_e U_e^\top V_{\text{tr}}^\text{H} \succeq V_{\text{tr}} \left(U_e \tilde{U}^\top + \tilde{U} U_e^\top - \tilde{U} \tilde{U}^\top \right) V_{\text{tr}}^\text{H}. \quad (32)$$

Inserting Inequality (32) in Inequality (29) leads to (30). \square

The bound derived in Lemma 3 is tight in case $\tilde{U} = U_e$. However, since U_e is unknown, we consider a candidate \tilde{U} of linearly independent amplitudes corresponding to their respective spectral lines. We later embed this relaxation in an iterative process to reduce conservatism. Furthermore, in (30), V_{tr} and Y_{tr} (in $\tilde{W} = Y_{\text{tr}} W$) are unknown. Hence, in what follows, suitable bounds are derived.

D. Bounds on transfer matrices

Denote

$$\tilde{V} = V_{\text{tr}} - \hat{V} \quad (33)$$

where the estimate

$$\hat{V} = [\hat{V}_1, \dots, \hat{V}_{n_\phi}] \in \mathbb{C}^{n_\phi \times L n_u} \quad (34)$$

is computed using the prior \hat{A}_0 and \hat{B}_0 (cf. Assumption 1). In Appendices A, B and C, we show how to compute a matrix $\Gamma_v \succ 0$ and a constant $\gamma_y > 0$ such that

$$\tilde{V} \tilde{V}^\text{H} \preceq \Gamma_v, \quad \|Y_{\text{tr}}\| \leq \gamma_y, \quad (35)$$

assuming $\theta_{\text{tr}} \in \Theta_0$.

Utilizing (35), we can derive a bound on \tilde{W} of the form $\|\tilde{W}\| \leq \|Y_{\text{tr}}\| \|W\|$. A bound on W can be determined since the each block on the diagonal of W is Gaussian. In particular, we have

$$\|W\| = \max_{i=1, \dots, n_\phi} \|\mathbf{w}(e^{j\omega_i})\|. \quad (36)$$

Since $\mathbf{w}(e^{j\omega_i}) \sim \mathcal{N}(0, \sigma_w^2 I)$, we have that $\|\mathbf{w}(e^{j\omega_i})\|^2 \sim \sigma_w^2 \chi_{n_x}^2$, and hence

$$\mathbb{P}(\|\mathbf{w}(e^{j\omega_i})\|^2 \leq l_1^2) = 1 - \delta, \quad \forall i = 1, \dots, L \quad (37)$$

with $l_1^2 = \sigma_w^2 \chi_{n_x}^2 (1 - \delta)$. Therefore, we have

$$\mathbb{P}(\|W\| \leq l_1) = 1 - \delta. \quad (38)$$

Using (35) and (38), we have

$$\tilde{W} \tilde{W}^\text{H} \preceq l^2 I := (\gamma_y l_1)^2 I. \quad (39)$$

The following lemma provides joint probabilistic bounds on \tilde{V} , Y_{tr} and W .

Lemma 4. *Let Assumption 1 hold. Then*

$$\mathbb{P}((\tilde{V} \tilde{V}^\text{H} \preceq \Gamma_v) \cap (\|Y_{\text{tr}}\| \leq \gamma_y) \cap (\|W\| \leq l_1)) \geq 1 - 2\delta. \quad (40)$$

Proof. From Lemma 1, since $\mathbb{P}(\theta_{\text{tr}} \in \Theta_0) \geq 1 - \delta$, the bounds in (35) hold with probability at least $1 - \delta$:

$$\begin{aligned} & \mathbb{P}((\tilde{V} \tilde{V}^\text{H} \preceq \Gamma_v) \cap (\|Y_{\text{tr}}\| \leq \gamma_y)) \geq \mathbb{P}(\theta_{\text{tr}} \in \Theta_0) \\ & \geq 1 - \delta. \end{aligned}$$

Hence,

$$\begin{aligned} & \mathbb{P}((\tilde{V} \tilde{V}^\text{H} \preceq \Gamma_v) \cap (\|Y_{\text{tr}}\| \leq \gamma_y) \cap (\|W\| \leq l_1)) \\ & \geq \mathbb{P}((\theta_{\text{tr}} \in \Theta_0) \cap (\|W\| \leq l_1)) \\ & \geq 1 - \mathbb{P}(\theta_{\text{tr}} \notin \Theta_0) - \mathbb{P}(\|W\| \not\leq l_1) \\ & \stackrel{(38)}{\geq} 1 - 2\delta \end{aligned} \quad (41)$$

wherein the penultimate inequality follows from De Morgan's law. \square

E. Final bound on the informativity of exploration

In the following theorem, we compute a lower bound \bar{D}_T on the informativity, i.e., the empirical covariance of the exploration data, before the process of exploration.

Theorem 1. *Let Assumption 1 hold. Suppose there exist matrices U_e and \bar{D}_T , and $\tau \geq 0$ such that $S_{\text{exploration}}(\epsilon, \tau, \tilde{U}, U_e, \hat{V}, l, \bar{D}_T, \Gamma_v) \succeq 0$ (31). Then, the application of the input (16) implies that with probability at least $1 - 2\delta$:*

$$D_T \succeq \bar{D}_T. \quad (42)$$

Proof. Since $\tilde{V} = \tilde{V}^\text{H}$, by using (33) and (35), we get

$$V_{\text{tr}} V_{\text{tr}}^\text{H} - V_{\text{tr}} \hat{V}^\text{H} - \hat{V} V_{\text{tr}}^\text{H} + \hat{V} \hat{V}^\text{H} \preceq \Gamma_v$$

which can be written as

$$\begin{bmatrix} V_{\text{tr}}^\text{H} \\ I \end{bmatrix}^\text{H} \begin{bmatrix} -I & \hat{V}^\text{H} \\ \hat{V} & \Gamma_v - \hat{V} \hat{V}^\text{H} \end{bmatrix} \begin{bmatrix} V_{\text{tr}}^\text{H} \\ I \end{bmatrix} \succeq 0. \quad (43)$$

Additionally, we have $\tilde{W} \tilde{W}^\text{H} \preceq l^2 I$ (39).

From Lemma 3, and by using (39), the following inequality implies that $D_T \succeq \bar{D}_T$:

$$\begin{aligned} & (1-\epsilon) \left(V_{\text{tr}} \left(U_e \tilde{U}^\top + \tilde{U} U_e^\top - \tilde{U} \tilde{U}^\top \right) V_{\text{tr}}^\text{H} \right) \\ & - \left(\frac{1-\epsilon}{\epsilon} \right) l^2 I - \frac{\bar{c} n_\phi}{T} \bar{D}_T \succeq 0. \end{aligned} \quad (44)$$

Furthermore, (44) can be written as

$$\begin{bmatrix} V_{\text{tr}}^\text{H} \\ I \end{bmatrix}^\text{H} \begin{bmatrix} (1-\epsilon)(U_e \tilde{U}^\top + \tilde{U} U_e^\top - \tilde{U} \tilde{U}^\top) & 0 \\ 0 & -(\frac{1-\epsilon}{\epsilon})l^2 I \\ & & -\frac{\bar{c} n_\phi}{T} \bar{D}_T \end{bmatrix} \begin{bmatrix} V_{\text{tr}}^\text{H} \\ I \end{bmatrix} \succeq 0. \quad (45)$$

From Lemma 4, Inequalities (43) and (39) hold jointly with probability $1 - 2\delta$. By using the S-procedure [30], (44) holds for all V_{tr} satisfying (43) if and only if (31) holds with $\tau \geq 0$.

Hence, if there exist U_e and \bar{D}_T satisfying (31), then (42) holds with probability at least $1 - 2\delta$. \square

As a result, we can pose the exploration problem of achieving a desired excitation \bar{D}_T with minimal input energy using the following SDP:

$$\begin{aligned} \inf_{U_e, \gamma_e, \tau} \quad & \gamma_e \\ \text{s.t.} \quad & S_{\text{energy-bound}}(\gamma_e, U_e) \succeq 0 \\ & S_{\text{exploration}}(\epsilon, \tau, \tilde{U}, U_e, \hat{V}, l, \bar{D}_T, \Gamma_v) \succeq 0 \\ & \tau \geq 0. \end{aligned} \quad (46)$$

Note that γ_e , U_e and τ are the only decision variables; ϵ , \tilde{U} and \bar{D}_T are user-defined, and \hat{V} , l and Γ_v are given by (34), (39) and (35), respectively. A solution of (46) gives us the parameters required for the implementation of the exploration input, i.e., $U_e = \text{diag}(a_1, \dots, a_L)$, which guarantees the desired excitation \bar{D}_T . The lower-bound \bar{D}_T also implies a lower bound $D_{\text{post}} \succeq \bar{D}_{\text{post}} = D_0 + \bar{D}_T$, and will be used to guarantee an uncertainty bound for dual control in Section VI. In order to reduce the suboptimality caused by the convex relaxation procedure, Problem (46) can be iterated multiple times by re-computing \tilde{U} for the next iteration as

$$\tilde{U} = U_e^* \quad (47)$$

wherein U_e^* is the solution from the previous iteration. The suboptimality of convex relaxation can be reduced by iterating until U_e does not change. Furthermore, γ_e is guaranteed to be non-increasing with each iteration since the previous optimal solution U_e^* remains feasible.

V. ROBUST GAIN-SCHEDULING DESIGN

After exploration as described in Section IV, the estimates \hat{A} and \hat{B} change due to the availability of new data. Since our goal is to design a stabilizing state-feedback controller that is influenced by the new estimates, the true system in (2) is modeled as a linear parameter varying (LPV) system, where the estimates \hat{A}_T , \hat{B}_T are measured online. The new estimates are utilized as a *scheduling variable* to design a gain-scheduling controller that ensures that the closed-loop system is stable while also satisfying a H_2 performance bound.

To account for the change in the estimates of the parameters after exploration, the system in (2) is rewritten as:

$$\begin{aligned} x_{k+1} &= A_{\text{tr}}x_k + B_{\text{tr}}u_k + w_k \\ &= \hat{A}_0x_k + \hat{B}_0u_k + (\hat{A}_T - \hat{A}_0)x_k + (\hat{B}_T - \hat{B}_0)u_k \\ &\quad + (A_{\text{tr}} - \hat{A}_T)x_k + (B_{\text{tr}} - \hat{B}_T)u_k + w_k. \end{aligned} \quad (48)$$

Designing a controller for (48) can be written in the form of a gain-scheduling problem with an uncertain signal $w^u = \Delta_u \phi$ and an online measurable signal $w^s = \Delta_s \phi$ with the corresponding scheduling and uncertainty blocks:

$$\begin{aligned} \Delta_s &= [\hat{A}_T - \hat{A}_0 \quad \hat{B}_T - \hat{B}_0], \\ \Delta_u &= [A_{\text{tr}} - \hat{A}_T \quad B_{\text{tr}} - \hat{B}_T]. \end{aligned} \quad (49)$$

The control input after exploration is defined as

$$u_k = K_x x_k + K_s w_k^s, \quad (50)$$

where we use the fact that w_k^s is known/measurable after exploration. The controller parameters K_x and K_s are designed such that the closed-loop system is robustly stable and the specified performance criterion is met. Since the estimates \hat{A}_T and \hat{B}_T affect both Δ_s and Δ_u , these blocks can be viewed as uncertain parameters, and the closed-loop uncertain system combining (3) and (48) can be written in the generalized plant form:

$$\begin{aligned} \begin{bmatrix} x_{k+1} \\ z_k^s \\ z_k^u \\ z_k \end{bmatrix} &= \begin{bmatrix} \hat{A}_0 + \hat{B}_0 K_x & I + \hat{B}_0 K_s & I & I \\ \begin{bmatrix} I \\ K_x \end{bmatrix} & \begin{bmatrix} 0 \\ K_s \end{bmatrix} & 0 & 0 \\ \begin{bmatrix} I \\ K_x \end{bmatrix} & \begin{bmatrix} 0 \\ K_s \end{bmatrix} & 0 & 0 \\ C + DK_x & DK_s & 0 & D_w \end{bmatrix} \begin{bmatrix} x_k \\ w_k^s \\ w_k^u \\ w_k \end{bmatrix}, \\ w_k^s &= \Delta_s z_k^s, \\ w_k^u &= \Delta_u z_k^u, \end{aligned} \quad (51)$$

where $w^s \rightarrow z^s$ is the scheduling channel and $w^u \rightarrow z^u$ is the uncertainty channel.

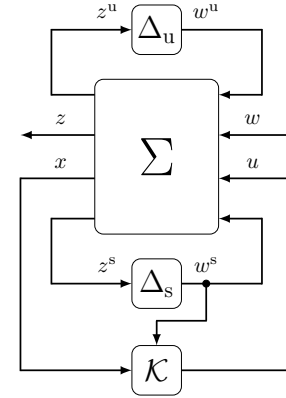


Fig. 2: Generalized plant view of the robust gain-scheduling problem [21].

As is apparent from Fig. 2, the closed-loop system has uncertainty and scheduling channels, affected by Δ_u and Δ_s , respectively. The latter block Δ_s is taken into account for the controller via w_k^s (cf. (50)), and hence plays the role of a scheduling variable. This accounts for changes in the mean of the system parameters through data gathered in the exploration phase that is available after exploration at time T .

Given this formulation and suitable bounds on the blocks Δ_s and Δ_u , the following lemma provides a matrix inequality to design a robust gain scheduling controller satisfying the performance specification defined in (4).

Lemma 5. *Suppose $\Delta_s \in \mathbf{\Delta}_s := \{\Delta : R_s - \Delta^\top \Delta \succ 0\}$, $\Delta_u \in \mathbf{\Delta}_u := \{\Delta : R_u - \Delta^\top \Delta \succ 0\}$, with $R_u, R_s \succ 0$. If there exist matrices K_s, M, N, Z and scalars $\lambda_s, \lambda_u > 0$ satisfying the matrix inequalities (52), then the closed loop (51) satisfies the H_2 performance bound γ_p (4) with $K_x = MN^{-1}$, i.e., $u_k = MN^{-1}x_k + K_s w_k^s$.*

$$S_{\text{gain-scheduling-1}}(K_s, M, N, \lambda_s, \lambda_u, R_s^{-1}, R_u^{-1}) = \left(\begin{array}{c|c} \begin{bmatrix} -N & 0 & 0 & 0 \\ 0 & -\lambda_s I & 0 & 0 \\ 0 & 0 & -\lambda_u I & 0 \\ 0 & 0 & 0 & -\gamma_p I \end{bmatrix} & * \\ \hline \begin{bmatrix} \hat{A}_0 N + \hat{B}_0 M & I + \hat{B}_0 K_s & I & I \\ \begin{bmatrix} N \\ M \\ N \\ M \\ 0 \end{bmatrix} & \begin{bmatrix} 0 \\ K_s \\ 0 \\ K_s \\ 0 \end{bmatrix} & 0 & 0 \end{bmatrix} & \begin{bmatrix} -N & 0 & 0 & 0 \\ 0 & -\frac{1}{\lambda_s} R_s^{-1} & 0 & 0 \\ 0 & 0 & -\frac{1}{\lambda_u} R_u^{-1} & 0 \\ 0 & 0 & 0 & -I \end{bmatrix} \end{array} \right) \prec 0 \quad (52a)$$

$$S_{\text{gain-scheduling-2}}(M, N, Z) = \begin{bmatrix} N & NC^\top + M^\top D^\top \\ CN + DM & Z \end{bmatrix} \succ 0 \quad (52b)$$

$$S_{\text{gain-scheduling-3}}(Z) = \text{trace}(Z) \leq \gamma_p \quad (52c)$$

The proof of Lemma 5 is provided in Appendix E. We later define R_s, R_u in terms of uncertainty bounds that affect the uncertain parameters Δ_s, Δ_u . For constants λ_s, λ_u , Inequalities (52) are LMIs. Hence, the matrix inequalities (52) can be efficiently solved using line-search like techniques for $(\lambda_s, \lambda_u) \in \mathbb{R}^2$.

The solution of (52) yields control parameters M, N and K_s which guarantee robust H_2 performance of the closed loop (51) for all bounded uncertainties $\Delta_s \in \mathbf{\Delta}_s, \Delta_u \in \mathbf{\Delta}_u$. In the next section, we combine the exploration strategy from Section IV, and the parametrized state-feedback controller based on gain-scheduling in the overall dual control strategy.

VI. DUAL CONTROL

In this section, we propose a dual control strategy by combining targeted exploration (Section IV), and robust gain-scheduling control (Section V).

A. Relationship between uncertain parameters

An important aspect of the proposed approach lies in establishing the relationship between the uncertainty bounds D_0, D_T , that influence the uncertain parameters Δ_u, Δ_s (49). Recall that $\theta_{\text{tr}} \in \Theta_0$ with high probability. In order to derive a bound on Δ_s that is less conservative than the bound in [21, Prop. 1], we carry out the following parameter projection.

Parameter projection: The estimate $\hat{\theta}_T = \text{vec}([\hat{A}_T, \hat{B}_T])$ is projected on Θ_0 (cf. (9)) as follows:

$$\tilde{\theta}_T = \Pi_{\Theta_0}(\hat{\theta}_T) := \arg \min_{\theta \in \Theta_0} \|\theta - \hat{\theta}_T\|_{(\overline{D}_{\text{post}} \otimes I_{n_x})}^2 \quad (53)$$

where $\overline{D}_{\text{post}} = D_0 + \overline{D}_T$ and $\tilde{\theta}_T = \text{vec}([\tilde{A}_T, \tilde{B}_T])$ is the projected estimate. We redefine Δ_s in terms of $(\tilde{A}_T, \tilde{B}_T)$ as

$$\Delta_s = [\tilde{A}_T - \hat{A}_0 \quad \tilde{B}_T - \hat{B}_0]. \quad (54)$$

From Lemma 1, we have $\mathbb{P}(\theta_{\text{tr}} \in \Theta_T) \geq 1 - \delta$ where

$$\Theta_T := \left\{ \theta : (\theta - \hat{\theta}_T)^\top (D_{\text{post}} \otimes I_{n_x}) (\theta - \hat{\theta}_T) \leq 1 \right\}, \quad (55)$$

with $D_{\text{post}} = D_0 + D_T$, and $\hat{\theta}_T$ is the estimate obtained after exploration (5). The following Lemma encapsulates the result of parameter projection and the bounds over uncertain parameters.

Lemma 6. *Let Assumption 1 hold. If there exist matrices U_e and \overline{D}_T satisfying the matrix inequality (31), then the following inequalities hold together with probability at least $1 - 3\delta$:*

$$\Delta_0^\top \Delta_0 \preceq D_0^{-1}, \quad (56)$$

$$\Delta_s^\top \Delta_s \preceq D_0^{-1}, \quad (57)$$

$$\Delta_u^\top \Delta_u \preceq \overline{D}_{\text{post}}^{-1}. \quad (58)$$

Proof. The proof is provided in four parts. In the first three parts of the proof, we prove (56)-(58) by assuming $\theta_{\text{tr}} \in (\Theta_0 \cap \Theta_T)$, where Θ_T is defined below, and $D_T \succeq \overline{D}_T$. In the last part, we then show that (56)-(58) hold jointly with probability at least $1 - 3\delta$.

Part I. Inequality (56) directly follows from $\theta_{\text{tr}} \in \Theta_0$ (cf. (9) - (12)).

Part II. By definition of $\tilde{\theta}_T$ in (53), from Lemma 1 we have $\tilde{\theta}_T \in \Theta_0$, which implies $[\tilde{A}_T, \tilde{B}_T] \in \mathbf{\Delta}_0$ (cf. (9)-(10)). Hence Inequality (57) holds with Δ_s according to (54).

Part III. Let

$$\overline{\Theta}_T := \left\{ \theta : (\theta - \hat{\theta}_T)^\top (\overline{D}_{\text{post}} \otimes I_{n_x}) (\theta - \hat{\theta}_T) \leq 1 \right\}. \quad (59)$$

Note that $D_T \succeq \overline{D}_T$ implies $D_{\text{post}} \succeq \overline{D}_{\text{post}}$. If $D_{\text{post}} \succeq \overline{D}_{\text{post}}$, then $\Theta_T \subseteq \overline{\Theta}_T$. Combining this with $\theta_{\text{tr}} \in \Theta_T$ yields $\theta_{\text{tr}} \in \overline{\Theta}_T$. Denote

$$\Theta_u := \left\{ \theta : (\theta - \tilde{\theta}_T)^\top (\overline{D}_{\text{post}} \otimes I_{n_x}) (\theta - \tilde{\theta}_T) \leq 1 \right\} \quad (60)$$

and correspondingly,

$$\Delta_u := \left\{ A, B : \begin{bmatrix} (A - \tilde{A}_T)^\top \\ (B - \tilde{B}_T)^\top \end{bmatrix}^\top \overline{D}_{\text{post}} \begin{bmatrix} (A - \tilde{A}_T)^\top \\ (B - \tilde{B}_T)^\top \end{bmatrix} \preceq I \right\}. \quad (61)$$

Since $\theta_{\text{tr}} \in \Theta_0$, then we have

$$\|\theta_{\text{tr}} - \tilde{\theta}_T\|_{(\overline{D}_{\text{post}} \otimes I_{n_x})} \leq \|\theta_{\text{tr}} - \hat{\theta}_T\|_{(D_{\text{post}} \otimes I_{n_x})}$$

given that the projection (53) is non-expansive (cf. Fig. 3). Hence, we have $\theta_{\text{tr}} \in \Theta_u$, which implies Inequality (58).

Part IV. We have

$$\begin{aligned}
& \mathbb{P}((\theta_{\text{tr}} \in (\Theta_0 \cap \Theta_T)) \cap (D_T \succeq \bar{D}_T)) \\
& \stackrel{(41)}{\geq} \mathbb{P}(\theta_{\text{tr}} \in (\Theta_0 \cap \Theta_T)) \cap (\|W\| \leq l_1) \\
& \geq 1 - \mathbb{P}(\theta_{\text{tr}} \notin \Theta_0) - \mathbb{P}(\theta_{\text{tr}} \notin \Theta_T) - \mathbb{P}(\|W\| \not\leq l_1) \\
& \stackrel{(55)}{\geq} 1 - 3\delta, \tag{62}
\end{aligned}$$

wherein the penultimate inequality follows from De Morgan's law. In Parts I-III, we showed that Inequalities (56)-(58) hold assuming $\theta_{\text{tr}} \in (\Theta_0 \cap \Theta_T)$ and $D_T \succeq \bar{D}_T$. In (62), we showed that $\theta_{\text{tr}} \in (\Theta_0 \cap \Theta_T)$ and $D_T \succeq \bar{D}_T$ hold jointly with probability at least $1 - 3\delta$, which implies that (56)-(58) hold with probability at least $1 - 3\delta$. \square

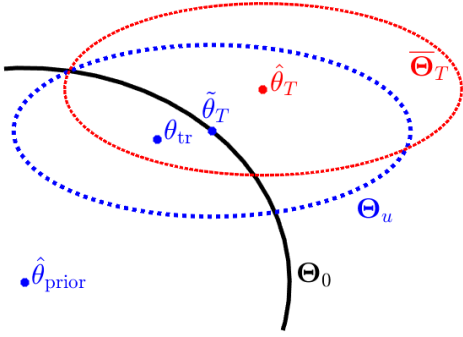


Fig. 3: Illustration of the sets from the proof of Lemma 6: $\Theta_0 = \Theta_s$, and Θ_u , the true parameters θ_{tr} , the initial parameter estimate $\hat{\theta}_{\text{prior}}$, the estimate resulting from exploration $\hat{\theta}_T$, and the projected estimate $\tilde{\theta}_T$.

The relationship between the different sets is illustrated in Figure 3. From Lemma 1, it is known that the true system parameters θ_{tr} are in some ellipse Θ_0 (9) around the initial parameter estimate $\hat{\theta}_{\text{prior}}$. After exploration, $\hat{\theta}_T$ is obtained and projected to $\tilde{\theta}_T$ (53). The projected $\tilde{\theta}_T$ is contained in the ellipse Θ_0 . This ensures the following bound on Δ_s : $\Delta_s^\top \Delta_s \preceq D_0^{-1}$ (57). This bound on Δ_s is enabled by parameter projection and is less conservative than the bound proposed in [21, Prop. 1]. The true system parameters θ_{tr} are in some ellipse Θ_u around the projected estimate $\tilde{\theta}_T$ with some probability. Finally, from Lemma 6, θ_{tr} lies in the intersection $\Theta_0 \cap \Theta_u$ with some probability which ensures bounds on Δ_0 and Δ_u (62). The satisfaction of these bounds enables the design of a robust gain-scheduled controller that guarantees H_2 performance (52), wherein we set $R_s^{-1} = D_0$ and $R_u^{-1} = \bar{D}_{\text{post}}$.

B. Proposed algorithm

The objective of the proposed dual control approach is to ensure that the designed controller satisfies the H_2 performance bound (4) with high probability, by incorporating a suitable *targeted* exploration strategy.

The following SDP combines the robust gain-scheduling problem in (52) and the exploration problem (46):

$$\inf_{U_e, \bar{D}_T, K_s, M, N, Z, \tau} \gamma_e \tag{63a}$$

$$\text{s.t. } S_{\text{energy-bound}}(\gamma_e, U_e) \succeq 0 \tag{63b}$$

$$S_{\text{exploration}}(\epsilon, \tau, \tilde{U}, U_e, \hat{V}, l, \bar{D}_T, \Gamma_v) \succeq 0 \tag{63c}$$

$$\tau \geq 0 \tag{63d}$$

$$S_{\text{gain-scheduling-1}}(K_s, M, N, \lambda_s, \lambda_u, R_s^{-1}, R_u^{-1}) \prec 0 \tag{63e}$$

$$S_{\text{gain-scheduling-2}}(M, N, Z) \succ 0 \tag{63f}$$

$$S_{\text{gain-scheduling-3}}(Z) \leq \gamma_p \tag{63g}$$

Note that the SDP depends on the prior information \hat{A}_0 , \hat{B}_0 , and D_0 (cf. Assumption 1), the desired H_2 performance specification γ_p , the exploration time T , candidate \tilde{U} , and bounds Γ_v , γ_y , l_1 . For fixed ϵ , λ_s , $\lambda_u > 0$, Problem (63) is an SDP comparable to [21, Eq. (28)]. Hence, the optimization problem can be solved efficiently using techniques like line-search or gridding for the variables ϵ , λ_s , $\lambda_u > 0$ with the SDP in an inner loop. Problem (63) is feasible only if the desired performance specification γ_p is achievable by the gain-scheduling-based controller.

The solution of this optimization problem yields the exploration input U_e , and parameters for the gain-scheduled controller K_s , M and N , which are subsequently used in the proposed sequential learning and control strategy. Recall that the exploration input is a linear combination of sinusoids, and can be implemented using the L selected frequencies $\omega_i \in \Omega_T$, $i = 1, \dots, L$, and their corresponding amplitudes $a_i = U_i$. The robust gain-scheduled controller can be implemented using K_s and $K_x = MN^{-1}$. Furthermore, the robust control LMIs (cf. Lemma 5) are contained in (63e), (63f) and (63g). These LMIs returns a common Lyapunov function $N \succ 0$ as well as controller parameters M , K_s which guarantee robust performance of the closed loop (51) for all uncertainties Δ_u, Δ_s satisfying $\Delta_u^\top \Delta_u \prec \bar{D}_{\text{post}}^{-1}$ and $\Delta_s^\top \Delta_s \prec D_0^{-1}$. Within this framework, the data obtained during the exploration phase is lower-bounded by $\bar{D}_T + D_0$. This suggests that the uncertainty characterized by \bar{D}_T for the robust controller design depends on the exploration phase through (63c). This couples the exploration phase and robust control, consequently resulting in a *dual effect* of the proposed controller.

Upon application of the exploration input determined by solving (63), new data is obtained. Combining the new data with the prior information, the MAP estimate (5) is used to obtain obtain improved/updated estimates \hat{A}_T , \hat{B}_T and a new bound D_T^{-1} on the uncertainty. Parameters θ_T are projected on Θ_0 , resulting in $\tilde{\theta}_T$ and corresponding to matrices \hat{A}_T , \hat{B}_T . This ensures that the uncertainty over the parameters (53) does not increase. Subsequently, after T time steps, the designed gain-scheduled controller with the new scheduling variable $\Delta_s = [\hat{A}_T - \hat{A}_0 \quad \hat{B}_T - \hat{B}_0]$ can be applied. Using (51), this controller can be explicitly written as a state feedback control

law K :

$$\begin{aligned}
u_k &= K_x x_k + K_s w_k^s & (64) \\
&= K_x x_k + K_s \left((\tilde{A}_T - \hat{A}_0) x_k + (\tilde{B}_T - \hat{B}_0) u_k \right) \\
&= \left(I_{n_u} - K_s (\tilde{B}_T - \hat{B}_0) \right)^{-1} \left(K_x + K_s (\tilde{A}_T - \hat{A}_0) \right) x_k \\
&=: K x_k.
\end{aligned}$$

Note that $(I - K_s(\tilde{B}_T - \hat{B}_0))$ is non-singular (with high probability) due to the equivalence in [25, Thm. 2]. The overall procedure is summarized in Algorithm 1.

Algorithm 1 Dual control using gain-scheduling

- 1: Use a Gaussian prior (cf. Assumption 1) to determine initial estimates \hat{A}_0, \hat{B}_0 and uncertainty bound D_0^{-1} .
 - 2: Specify confidence level $\delta \in (0, 1)$, H_2 performance index γ_p (4), exploration length T and L frequencies.
 - 3: Compute scalar l_1 (37). Compute bounds Γ_v and γ_y (35), and via methods described in Appendix A and B.
Alternative: Set $\beta \ll 1$, e.g., $\beta = 10^{-10}$, and compute bound Γ_v and γ_y (35) via the scenario approach as described in Appendix C.
 - 4: Select initial candidate \tilde{U} (47).
 - 5: Solve the optimization problem (63) for different values $\epsilon, \lambda_s, \lambda_u > 0$ (e.g., via line-search in an outer loop).
 \Rightarrow Sinusoidal exploration sequence amplitudes $a_i = 2U_i$ corresponding to their frequencies ω_i (cf. (16)).
 \Rightarrow Gain-scheduled controller parameters $K_s, K_x = MN^{-1}$ (cf. (64)).
 - 6: Apply the exploration input as in (16) for $k = 0, \dots, T-1$.
 - 7: Update estimates \hat{A}_T, \hat{B}_T using new data (c.f. MAP estimation (5)) and obtain projected parameters \tilde{A}_T, \tilde{B}_T (53).
 - 8: Compute the state-feedback K dependent on \tilde{A}_T, \tilde{B}_T (64).
 - 9: Apply the feedback $u_k = Kx_k, k \geq T$.
-

C. Theoretical analysis

The following result proves that Algorithm 1 leads to a controller with closed-loop guarantees.

Theorem 2. *Let Assumption 1 hold. Suppose Problem (63) is feasible, and Algorithm 1 is applied. Then, with probability $1 - 3\delta$, the closed-loop system (51) with $u_k = Kx_k$ (64) satisfies the H_2 performance² bound γ_p (4).*

Proof. Firstly, we recall that Lemma 5 guarantees the performance bound (4), assuming suitable bounds on Δ_s and Δ_u . Then, we show that the exploration inequalities in combination with parameter projection in (53) ensure the bounds on Δ_s and Δ_u .

Part I. According to Lemma 5, the satisfaction of the robust control LMIs in (52) guarantees that the robust gain-scheduled controller $u_k = MN^{-1}x_k + K_s w_k^s$ ensures the H_2

²In case the constants Γ_v and γ_y are both computed using the scenario approach (cf. Appendix C), then each constant is only valid with confidence of $1 - \beta$ and correspondingly the robust performance bound only holds with probability $1 - 3\delta - 2\beta$.

performance bound (4), if $\Delta_s^\top \Delta_s \preceq D_0^{-1}$, $\Delta_u^\top \Delta_u \preceq \overline{D}_{\text{post}}^{-1}$. Thus, only the bounds $\Delta_s^\top \Delta_s \preceq D_0^{-1}$, $\Delta_u^\top \Delta_u \preceq \overline{D}_{\text{post}}^{-1}$ remain to be shown.

Part II. Lemma 6 shows that these bounds hold jointly with probability at least $1 - 3\delta$. (62)

Hence, the closed-loop system (51) with $u_k = Kx_k$ (64) satisfies the performance bound (4) with probability $1 - 3\delta$. \square

This result summarizes the theoretical properties of the proposed dual control approach, ensuring a desired performance specification (4) using a targeted exploration strategy.

D. Discussion

In what follows, we discuss the main features of the proposed approach as well as connections to existing works.

Summary - proposed approach: The proposed approach, as outlined in Algorithm 1, yields a sequential learning and control strategy jointly from SDP (63): (i) a harmonic exploration input to generate data for maximum a posteriori estimation; (ii) a linear state-feedback (exploitation) which is implemented after exploration. The resulting state-feedback explicitly depends on the generated data in terms of the mean estimate and (with high probability) guarantees stability and performance (cf. Theorem 2). In general, direct state measurement, which is required for state-feedback, is a practical limitation. However, the assumption of i.i.d. process noise that is normally distributed with zero mean and known variance, and direct state measurement, allow the usage of standard MAP estimation which simplifies the exposition of the main results and supports the description of non-asymptotic uncertainty bounds. The lower-bound on excitation that is derived is comparable to the Fisher information matrix [31], with the key difference that in the design process that follows, uncertainty arising from prior information is robustly accounted for. The proposed control strategy has a dual effect in the sense that the choice of the harmonic exploration input shapes the uncertainty bound of the MAP estimate after exploration (cf. Lemma 1 & Theorem 1), which enters in the robust performance bound during exploitation (cf. Lemma 5). A main technical tool for establishing this link is the theory of spectral lines applied to the harmonic exploration (cf. Section IV). As a result, the proposed exploration is *targeted* in the sense that the amplitudes at different frequencies influence both the magnitude and the shape/direction of the uncertainty after exploration, and hence the uncertainty that is accounted for in the (robust) control design. Our dual control approach uses Problem (63), which minimizes the energy of the exploration input such that a specified performance can be guaranteed for the closed loop after the exploration phase. Note that the presented theoretical results can be equally used to re-design a robust controller after exploration, however, with the drawback of re-solving an LMI online. With trivial modifications, it is also possible to solve the converse problem, i.e., optimizing the closed-loop performance after exploration subject to a constraint on the exploration energy.

Related approaches: The proposed dual control algorithm is similar to, and inspired by, recent robust dual control

approaches [18], [19], albeit with two crucial differences that are discussed as follows.

Firstly, in the exploration phase, we consider *harmonic* inputs of the form $u_k = \sum_{i=1}^L a_i \cos(\omega_i k)$, whereas [18], [19], [21] suggest inputs $u_k = Kx_k + v_k$ with a matrix K and a zero-mean Gaussian random variable v_k . The frequencies ω_i in the harmonic input signal are specified a priori, and allow for an intuitive tuning based on possible prior knowledge about the system. Subsequently, the proposed dual control approach determines the corresponding amplitudes a_i , weighting the frequency components to achieve a targeted uncertainty reduction. Most importantly, the influence of the exploration input on the uncertainty bound after exploration can be quantified *a priori*, in a rigorous manner as derived in Section III-B, using the theory of spectral lines [23]. On the contrary, the bounds obtained by [18], [19], [21] do *not* yield any guarantees for the actual exploration since the empirical covariance is approximated in a heuristic way via the worst-case covariance.

Secondly, in the exploitation phase, we consider a *gain-scheduling controller*, where the difference of the parameter estimates before and after exploration plays the role of the scheduling parameter. This enables us to provide a priori performance and stability guarantees. On the contrary, [18] and [19] consider the simplification that the estimate after exploration is equal to initial estimate. Given that the initial estimate is uncertain, [18] and [19] require a re-design step after exploration. Furthermore, such an additional online design step, which could be equivalently added in our proposed approach to further improve performance, implies that the exploration is not directly targeted to the final robust design problem, and no *a priori* guarantees can be given. We note that a similar gain-scheduling approach to robust dual control was also suggested in our preliminary work [21], however, employing a random exploration strategy without excitation guarantees and satisfying a quadratic performance bound. Furthermore, in [21], we consider a random exploration input as in [18] and [19], and hence the resulting guarantees were only valid under restrictive assumptions (cf. [21, Assumption 2]).

Finally, we note that the considered control problem could also be addressed using results from regret analysis and sample complexity bounds of LQR design based on system identification. For example, in [32], a random excitation is followed by the least-squares estimate and a robust LQR design. This also provides performance/regret bounds with respect to the optimal policy in dependence of the number of roll-outs, i.e., numerous trials with re-start. In contrast to the proposed approach, the exploration is not targeted, and in general, the guarantees are qualitative in nature, i.e., in the limit of multiple roll-outs, the performance approaches the optimum, but, sharp performance specifications for the first roll-outs cannot be given.

VII. NUMERICAL EXAMPLE

In this section, we demonstrate the practical applicability of the proposed sequential robust dual control approach through a numerical example, which is ‘hard to learn’. Numerical simulations were performed on MATLAB using CVX [33]

in conjunction with the default SDP solver SDPT3. First, we illustrate the benefits of the proposed targeted exploration strategy (46) compared to a common random exploration strategy (Section IV). Subsequently, we implement the overall dual control strategy (Algorithm 1) and demonstrate the trade-off between exploration energy and performance achieved after exploration (Section VI).

A. Problem setup

We consider a linear system (2) with $\sigma_w^2 = 1$ and

$$A_{\text{tr}} = \begin{bmatrix} 0.49 & 0.49 & 0 & 0 \\ 0 & 0.49 & 0.49 & 0 \\ 0 & 0 & 0.49 & 0.49 \\ 0 & 0 & 0 & 0.49 \end{bmatrix}, B_{\text{tr}} = \begin{bmatrix} 0 \\ 0 \\ 0 \\ 0.49 \end{bmatrix} \quad (65)$$

which belongs to a class of linear systems identified as ‘hard to learn’ [34]. The generalized error (3) is characterized by the known matrices $C = I$ and $D_u = 0$. We generate one random noise sequence $w_k \sim \mathcal{N}(0, 1)$ for the exploration time horizon $T = 100$, which is used for all the following simulations. We consider a Gaussian prior (cf. Assumption 1) with initial estimate $\hat{\theta}_{\text{prior}}$ and an initial uncertainty bound $D_0^{-1} = 5 \cdot 10^{-3} I$. The estimate $\hat{\theta}_{\text{prior}}$ is sampled randomly such that $(\hat{\theta}_{\text{prior}} - \theta_{\text{tr}})^\top (D_0 \otimes I_{n_x}) (\hat{\theta}_{\text{prior}} - \theta_{\text{tr}}) \leq 1$. We set $\epsilon = 0.5$ and select the probability of violation $\delta = 0.01$. The constants Γ_v, l are computed using the scenario approach (cf. Appendix C) with confidence level $\beta = 10^{-10}$.

B. Targeted exploration

In this section, we demonstrate the targeted exploration strategy as described in Section IV. In addition, we compare the targeted exploration strategy with a random exploration strategy that applies normally distributed inputs, i.e., the inputs $u_k \sim \mathcal{N}(0, 1)$. For a fair comparison, the random exploration inputs are scaled such that both strategies apply inputs with the same energy for exploration. We then evaluate and compare the level of excitation achieved.

In the context of targeted exploration, the objective is to ensure a given lower bound on excitation $D_T \succeq \bar{D}_T$, and targeted exploration inputs are obtained by solving the exploration problem (46). In our simulations, we set $T = 100$ and select $L = 10$ frequencies from the set Ω_{100} to yield $\omega_i = \{0, 0.1, 0.2, 0.3, 0.4, 0.5, 0.6, 0.7, 0.8, 0.9\}$, $i = 1, \dots, L$. The solution of (46) provides the resulting amplitudes a_i , $i = 1, \dots, L$ corresponding to the sinusoids with frequencies ω_i , $i = 1, \dots, L$. Given T , a_i and ω_i , the input signal (16) and its energy $\sum_{k=1}^T u_k^2$ can be computed. In the context of random exploration, we use normally distributed inputs.

In our simulations, we implement the proposed targeted exploration and random exploration for different initial uncertainty bounds D_0^{-1} . Due to the chained structure of A_{tr} with weakly-coupled states, it is difficult to excite the first state. Hence, we compare the excitation achieved by targeted and random exploration corresponding to the first state, i.e., the (1,1)-element of D_T denoted by $D_{T_{11}}$. We impose a constraint on $D_{T_{11}}$ by setting $\bar{D}_{T_{11}} \geq 10^6$. For a trial, we multiply the initial excitation bound D_0 by a factor α_i to

achieve $D_{0_i} = \alpha_i D_0$. We randomly sample a prior estimate $\hat{\theta}_{\text{prior},i}$ such that $(\hat{\theta}_{\text{prior},i} - \theta_{\text{tr}})^\top (D_{0_i} \otimes I_{n_x}) (\hat{\theta}_{\text{prior},i} - \theta_{\text{tr}}) \leq 1$, and compute the corresponding constants $\Gamma_{v,i}$ and l_i via the scenario approach (cf. Appendix C). We run 10 trials for each of the following values $\alpha_i \in \{10^0, 10^1, 10^2, 10^3, 10^4\}$ wherein each trial uses a different randomly sampled initial estimate $\hat{\theta}_{\text{prior}}$ and a different sequence of random inputs for random exploration. Each trial comprises: (i) determining the initial excitation bound D_{0_i} , prior estimate $\hat{\theta}_{\text{prior},i}$, and the corresponding constants $\Gamma_{v,i}$ and l_i , (ii) solving the exploration problem (46) to obtain targeted exploration inputs, and (iii) generating random exploration inputs with the same energy as the targeted inputs. We iterate Problem (46) over \tilde{U} (47), as described in Section IV-E to reduce the suboptimality of convex relaxation. Given the targeted and random exploration inputs, we get observed data sets from 10 trials corresponding to each α_i . From the datasets, we compute the mean value of finite excitations achieved by targeted exploration $D_{T_{T,i,11}}$ and random exploration $D_{T_{R,i,11}}$. From Fig. 4, it can be observed that the targeted exploration inputs achieve the desired excitation for all tested initial uncertainty levels, i.e., $D_{T_{T,i,11}} \geq 10^6$ for all trials. The achieved excitation is higher than the desired excitation due to inherent conservatism of the targeted exploration strategy, which utilizes worst-case bounds Γ_v and l . The strategy is more conservative for large initial uncertainty (small α). On the other hand, random exploration achieves significantly smaller excitation with the same energy by a factor of approximately 10. Furthermore, random exploration has a large variance in the achieved exploration due to the stochasticity introduced by the random inputs. Hence, targeting the exploration with respect to the desired excitation can have enormous advantages over random exploration.

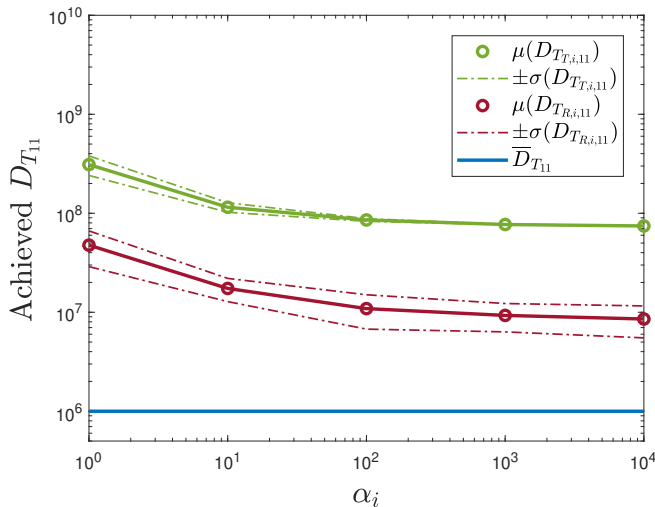


Fig. 4: Illustration of (i) the mean and standard deviation of the excitation achieved by targeted exploration $D_{T_{T,i,11}}$, and by random exploration $D_{T_{R,i,11}}$, for different values of α_i that scales the initial uncertainty bound D_0 , and (ii) the desired excitation $\bar{D}_{T_{11}} = 10^6$.

C. Dual control with robust gain-scheduling

In this section, we use the proposed dual control strategy to study the trade-off between the desired H_2 performance and the resulting exploration energy γ_e (17). We consider again an initial uncertainty bound, i.e., $D_0^{-1} = 5 \cdot 10^{-3} I$ and a fixed initial estimate $\hat{\theta}_{\text{prior}}$ satisfying $(\hat{\theta}_{\text{prior}} - \theta_{\text{tr}})^\top (D_0 \otimes I_{n_x}) (\hat{\theta}_{\text{prior}} - \theta_{\text{tr}}) \leq 1$. For H_2 performance, we consider a $\gamma_p > 0$ (Def. 1). In order to determine the efficacy of the proposed dual controller, we additionally determine the performance of a nominal H_2 controller with exact model knowledge, which is denoted by $\underline{\gamma}_p = 2.65$, and the performance of a robust H_2 controller computed based on the initial uncertainty bound D_0^{-1} , which is denoted by $\bar{\gamma}_p = 3.05$. We solve Problem (63) for different values of γ_p in the interval $[\underline{\gamma}_p, \bar{\gamma}_p]$. From Fig. 5, it can be observed as we want to achieve better performance (decrease γ_p), the required exploration energy γ_e increases. There exists a large range of γ_p where we can incrementally achieve better performance by increasing exploration energy. However, there exists a minimal performance $\gamma_p \approx 2.85$ which we can guarantee a priori with the proposed approach, even with arbitrarily large exploration energy. The fact that this is larger than the ideal performance $\underline{\gamma}_p = 2.65$ is partially due to the conservatism of the robust gain-scheduling synthesis based on a common Lyapunov function.

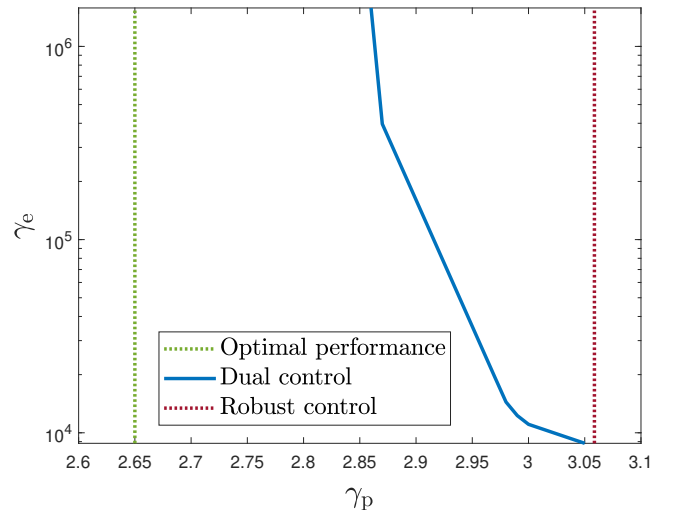


Fig. 5: Illustration of the exploration energy γ_e required to achieve a certain H_2 performance γ_p . For comparison, the H_2 performance of a robust controller based on the initial uncertainty bound D_0^{-1} , and the optimal H_2 performance based on true system knowledge are provided.

For fixed values of ϵ , λ_s , and λ_{ii} , the average execution time of Problem (63) over 10 trials, with and without iterations over \tilde{U} is 2.74 seconds and 0.85 seconds, respectively. In the considered numerical example, satisfactory performance was observed for fixed $\epsilon = 0.5$, and line-search over λ_s and λ_{ii} . In the numerical example, the line-search involved 10 iterations. The average execution time for solving Problem (63) in a loop with line-search, over 10 trials, is approximately 28 seconds. In general, Problem (63) is a standard SDP, and the computational

effort scales polynomially with the dimension of the state n_x and the control input n_u . The simulations were carried out on a system with an Intel(R) Core(TM) i7-9750H CPU @ 2.60GHz Processor and 16.0 GB RAM.

Overall, the simulation results corroborate the benefits of the proposed dual-control strategy. Given an initial prior and uncertainty bound, the targeted exploration strategy guarantees an *a priori* lower bound on excitation, which in turn influences the uncertainty bound over model parameters after exploration. Furthermore, dual control with gain-scheduling demonstrates the *targeted* nature of the exploration inputs, i.e., exploration is only carried out in order to improve the accuracy of system parameters and increase performance beyond the performance of a robust controller with knowledge of initial uncertainty.

VIII. CONCLUSION

In this article, we presented a sequential dual control strategy that involves a targeted exploration phase with harmonic inputs that can guarantee *a priori* excitation bounds, and a robust control phase based on gain scheduling that can guarantee H_2 performance after exploration. To simplify the exposition, we consider Schur stable systems. The main technical tool used to design the exploration phase is the theory of spectral lines. The amplitudes of the harmonic inputs are optimized so as to shape the uncertainty bound of the parameter estimates after exploration, which are accounted for by the controller based on gain scheduling, and thereby encapsulate the dual effect. We have demonstrated the applicability of the proposed dual control strategy, and clear benefits of targeted exploration, with numerical application to a system from a class that is ‘hard to learn’.

In summary, to the best knowledge of the authors, the presented approach provides the first solution of the *robust dual control problem*, which is (i) computationally tractable, and (ii) links a targeted exploration with an exploitation phase yielding robust guarantees without resorting to approximations or heuristics to mimic a dual effect. We expect that the practical performance can be further improved by using prior knowledge to pick appropriate frequencies in the exploration inputs.

APPENDIX A BOUND ON $\tilde{V}\tilde{V}^H$

In order to determine a bound of the form $\tilde{V}\tilde{V}^H \preceq \Gamma_v$, we first determine a bound on $\|\tilde{V}\|$ based on the sub-matrices of \tilde{V} . The matrix $\tilde{V} = V_{\text{tr}} - \hat{V} \in \mathbb{C}^{n_\phi \times L n_u}$ can be denoted in terms of its sub-matrices as $\tilde{V} = [\tilde{V}_1, \dots, \tilde{V}_L] = [V_1 - \hat{V}_1, \dots, V_L - \hat{V}_L]$.

Proposition 1. *Suppose $\|\tilde{V}_i\| \leq \bar{\gamma}_v, \forall i = 1, \dots, L$, then $\|\tilde{V}\| \leq \bar{\gamma}_v \sqrt{L}$.*

Proof. For $x = [x_1^\top, \dots, x_L^\top] \in \mathbb{C}^{L n_u}$, we have:

$$\begin{aligned} \|\tilde{V}\| &= \sup_{\|x\| \leq 1} \|\tilde{V}x\| = \sup_{\|x\| \leq 1} \|\tilde{V}_1 x_1 + \dots + \tilde{V}_L x_L\| \\ &\leq \sup_{\|x\| \leq 1} \sum_{i=1}^L \|\tilde{V}_i x_i\| \\ &\leq \bar{\gamma}_v \sup_{\|x\| \leq 1} \sum_{i=1}^L \|x_i\| = \bar{\gamma}_v \sqrt{L} \end{aligned}$$

where the penultimate inequality results from the triangle inequality property of the operator norm, and the final inequality results from the Cauchy-Schwarz inequality. \square

The matrices \tilde{V}_i are components of the transfer matrix of the following open loop system evaluated at frequencies $\omega_i \in \Omega_T, i = 1, \dots, L$:

$$\begin{aligned} \xi_{k+1} &= \begin{bmatrix} \hat{A}_0 & 0 \\ 0 & A_{\text{tr}} \end{bmatrix} \xi_k + \begin{bmatrix} \hat{B}_0 \\ B_{\text{tr}} \end{bmatrix} u_k \\ z_k &= \begin{bmatrix} I & -I \\ 0 & 0 \end{bmatrix} \xi_k + \begin{bmatrix} 0 \\ I \end{bmatrix} u_k \end{aligned} \quad (66)$$

where $\xi_k = \begin{bmatrix} \hat{x}_k \\ x_k \end{bmatrix}$. The prior uncertainty block is denoted as

$$\Delta_0 = [A_{\text{tr}} - \hat{A}_0 \quad B_{\text{tr}} - \hat{B}_0]. \quad (67)$$

Given $\Delta_0^\top \Delta_0 \preceq D_0^{-1}$ (cf. Assumption 1 and Lemma 1), we can compute $\bar{\gamma}_v$ such that $\|\tilde{V}_i\| \leq \bar{\gamma}_v$ using the (robust) H_∞ -norm, which is equal to the ℓ_2 -gain of the system (66). The ℓ_2 -gain for the channel $u \rightarrow z$ is guaranteed to be robustly smaller than $\bar{\gamma}_v$ if, for $P_p = \begin{pmatrix} -\bar{\gamma}_v I & 0 \\ 0 & \frac{1}{\bar{\gamma}_v} I \end{pmatrix}$, the following inequality holds for some $\epsilon > 0$ (cf. [35]):

$$\sum_{k=0}^{\infty} \begin{pmatrix} u_k \\ z_k \end{pmatrix}^\top P_p \begin{pmatrix} u_k \\ z_k \end{pmatrix} \leq -\epsilon \sum_{k=0}^{\infty} u_k^\top u_k. \quad (68)$$

Accounting for the prior uncertainty bound and re-writing (66) in the standard form, we get

$$\begin{bmatrix} \xi_{k+1} \\ z_k^u \\ z_k \end{bmatrix} = \begin{bmatrix} \begin{bmatrix} \hat{A}_0 & 0 \\ 0 & \hat{A}_0 \end{bmatrix} & \begin{bmatrix} 0 \\ I \end{bmatrix} & \begin{bmatrix} \hat{B}_0 \\ \hat{B}_0 \end{bmatrix} \\ \begin{bmatrix} 0 & I \\ 0 & 0 \end{bmatrix} & 0 & \begin{bmatrix} 0 \\ I \end{bmatrix} \\ \begin{bmatrix} I & -I \\ 0 & 0 \end{bmatrix} & 0 & \begin{bmatrix} 0 \\ 1 \end{bmatrix} \end{bmatrix} \begin{bmatrix} \xi_k \\ w_k^u \\ u_k \end{bmatrix}, \quad (69)$$

$$w_k^u = \Delta_0 z_k^u.$$

Given (69), $\bar{\gamma}_v$ is a valid H_∞ -norm bound if there exists an $X \succ 0$, a multiplier P_p of the form given earlier, and some

scalar $\lambda_v > 0$ such that

$$\begin{bmatrix} * \\ * \\ * \\ * \\ * \end{bmatrix}^\top \left[\begin{array}{ccc|ccc} -X & 0 & 0 & 0 & 0 & 0 \\ 0 & X & 0 & 0 & 0 & 0 \\ \hline 0 & 0 & \lambda_v P_u & 0 & 0 & 0 \\ 0 & 0 & 0 & 0 & 0 & 0 \\ \hline 0 & 0 & 0 & 0 & 0 & P_p \end{array} \right] \times \left[\begin{array}{ccc|ccc} I & 0 & 0 & & & \\ \hline \begin{bmatrix} \hat{A}_0 & 0 \\ 0 & \hat{A}_0 \end{bmatrix} & \begin{bmatrix} 0 \\ 1 \end{bmatrix} & \begin{bmatrix} \hat{B}_0 \\ \hat{B}_0 \end{bmatrix} & & & \\ \hline 0 & I & 0 & & & \\ \hline \begin{bmatrix} 0 & I \\ 0 & 0 \end{bmatrix} & 0 & \begin{bmatrix} 0 \\ I \end{bmatrix} & & & \\ \hline 0 & 0 & I & & & \\ \hline \begin{bmatrix} I & -I \\ 0 & 0 \end{bmatrix} & 0 & \begin{bmatrix} 0 \\ I \end{bmatrix} & & & \end{array} \right] \prec 0, \quad (70)$$

where $P_u = \begin{bmatrix} -I & 0 \\ 0 & D_0^{-1} \end{bmatrix}$ (cf. [25]). By defining $X = N^{-1}$ and multiplying the Schur complement of (70) from left and right by $\text{diag}(N, I, I)$, we get:

$$\left[\begin{array}{ccc|ccc} \begin{bmatrix} -N & 0 & 0 \\ 0 & -\lambda_v I & 0 \\ 0 & 0 & -\bar{\gamma}_v I \end{bmatrix} & & & & & * \\ \hline \begin{bmatrix} \hat{A}_0 & 0 \\ 0 & \hat{A}_0 \end{bmatrix} N & \begin{bmatrix} 0 \\ I \end{bmatrix} & \begin{bmatrix} \hat{B}_0 \\ \hat{B}_0 \end{bmatrix} & & & \\ \hline \begin{bmatrix} 0 & I \\ 0 & 0 \end{bmatrix} N & 0 & \begin{bmatrix} 0 \\ I \\ 0 \end{bmatrix} & & & \\ \hline \begin{bmatrix} I & -I \\ 0 & 0 \end{bmatrix} N & 0 & \begin{bmatrix} 0 \\ I \end{bmatrix} & & & \\ \hline \begin{bmatrix} -N & 0 & 0 \\ 0 & -\frac{1}{\lambda_v} D_0 & 0 \\ 0 & 0 & -\bar{\gamma}_v I \end{bmatrix} & & & & & \end{array} \right] \prec 0 \quad (71)$$

A solution of (71) gives $\bar{\gamma}_v$ from which we can compute the bound

$$\|\tilde{V}\| \leq \bar{\gamma}_v \sqrt{L}. \quad (72)$$

Hence,

$$\tilde{V}\tilde{V}^H \preceq \Gamma_v := \bar{\gamma}_v^2 L I \quad (73)$$

holds with probability at least $1 - \delta$ since the bound on the prior uncertainty block holds with probability at least $1 - \delta$, i.e. $\mathbb{P}(\Delta_0^\top \Delta_0 \preceq D_0^{-1}) \geq 1 - \delta$ (cf. Assumption 1 and Lemma 1).

APPENDIX B BOUND ON $\|Y_{\text{tr}}\|$

A bound on $\|Y_{\text{tr}}\|$ can be derived in terms of the bounds on its sub-matrices as in Proposition 1 (cf. Appendix A). Matrices $\|Y_i\|$ are the transfer matrix of the following open loop system evaluated at frequencies $\omega_i \in \Omega_T$, $i = 1, \dots, L$:

$$\begin{aligned} x_{k+1} &= A_{\text{tr}} x_k + w_k \\ z_k &= x_k. \end{aligned} \quad (74)$$

Hence, the bound $\bar{\gamma}_y$ is the H_∞ norm of its transfer matrix, which is equal to the ℓ_2 -gain of the system. The ℓ_2 -gain for the channel $w \rightarrow z$ is guaranteed to be robustly smaller than $\bar{\gamma}_y$

if, for $P_p = \begin{pmatrix} -\bar{\gamma}_y I & 0 \\ 0 & \frac{1}{\bar{\gamma}_y} I \end{pmatrix}$, the following inequality holds for some $\epsilon > 0$ (cf. [35]):

$$\sum_{k=0}^{\infty} \begin{pmatrix} w_k \\ z_k \end{pmatrix}^\top P_p \begin{pmatrix} w_k \\ z_k \end{pmatrix} \leq -\epsilon \sum_{k=0}^{\infty} w_k^\top w_k. \quad (75)$$

Since A_{tr} is unknown, we first re-write (74) as

$$\begin{aligned} x_{k+1} &= \hat{A}_0 x_k + (A_{\text{tr}} - \hat{A}_0) x_k + w_k \\ z_k &= x_k. \end{aligned} \quad (76)$$

The prior uncertainty block is denoted as

$$\Delta_0 = [A_{\text{tr}} - \hat{A}_0 \quad B_{\text{tr}} - \hat{B}_0]. \quad (77)$$

From Assumption 1 and Lemma 1, we have $\mathbb{P}(\Delta_0^\top \Delta_0 \preceq D_0^{-1}) \geq 1 - \delta$. Accounting for the prior uncertainty bound and re-writing (76) in the standard form, we get

$$\begin{bmatrix} x_{k+1} \\ z_k^u \\ z_k \end{bmatrix} = \begin{bmatrix} \hat{A}_0 & I & I \\ I & 0 & 0 \\ 0 & 0 & 0 \end{bmatrix} \begin{bmatrix} x_k \\ w_k^u \\ w_k \end{bmatrix}, \quad (78)$$

$$w_k^u = \Delta_0 z_k^u.$$

Given (78), $\bar{\gamma}_y$ is a valid H_∞ bound if there exists an $X \succ 0$, a multiplier P_p of the form given earlier, and a positive scalar $\lambda_y > 0$ such that

$$\begin{bmatrix} * \\ * \\ * \\ * \\ * \end{bmatrix}^\top \left[\begin{array}{ccc|ccc} -X & 0 & 0 & 0 & 0 & 0 \\ 0 & X & 0 & 0 & 0 & 0 \\ \hline 0 & 0 & \lambda_y P_u & 0 & 0 & 0 \\ 0 & 0 & 0 & 0 & 0 & 0 \\ \hline 0 & 0 & 0 & 0 & 0 & P_p \end{array} \right] \begin{bmatrix} I & 0 & 0 \\ \hat{A}_0 & I & I \\ 0 & I & 0 \\ \hline I & 0 & 0 \\ 0 & 0 & I \\ I & 0 & 0 \end{bmatrix} \prec 0 \quad (79)$$

where $P_u = \begin{bmatrix} -I & 0 \\ 0 & D_0^{-1} \end{bmatrix}$ [25]. By defining $X = N^{-1}$ and multiplying the Schur complement of (79) from left and right by $\text{diag}(N, I, I)$, we get:

$$\left[\begin{array}{ccc|ccc} \begin{bmatrix} -N & 0 & 0 \\ 0 & -\lambda_y I & 0 \\ 0 & 0 & -\bar{\gamma}_v I \end{bmatrix} & & & & & * \\ \hline \begin{bmatrix} \hat{A}_0 N & I & I \\ N & 0 & 0 \\ 0 & 0 & 0 \end{bmatrix} & & & \begin{bmatrix} -N & 0 & 0 \\ 0 & -\frac{1}{\lambda_y} D_0 & 0 \\ 0 & 0 & -\bar{\gamma}_v I \end{bmatrix} & & \end{array} \right] \prec 0 \quad (80)$$

A solution of (80) gives $\bar{\gamma}_y$, from which we can compute the bound

$$\|\tilde{Y}\| \leq \gamma_y := \bar{\gamma}_y \sqrt{L} \quad (81)$$

which holds with probability at least $1 - \delta$.

APPENDIX C SAMPLE-BASED CONSTANTS

Bounds Γ_v and γ_y in (35) are derived in Appendices A-B. However, these bounds can be conservative, and in what follows, we propose sample-based bounds that can be determined using the ‘scenario’ approach [36].

Scenario approach to estimate Γ_v : The bound Γ_v on the uncertain term $\tilde{V}\tilde{V}^H$ in Appendix A is computed under the assumption that $\theta_{\text{tr}} \in \Theta_0$. A tighter upper bound Γ_v can be computed by directly estimating an upper bound on $\tilde{V}\tilde{V}^H$. In order to estimate Γ_v , we generate N_s samples of $\text{vec}(A_i, B_i) = \theta_i \in \Theta_0$, $i = 1, \dots, N_s$, from the multivariate normal distribution with mean $\hat{\theta}_{\text{prior}}$ and covariance $\Sigma_{\theta, \text{prior}}$ (cf. Assumption 1). Given a probability of violation δ , and the number of uncertain decision variables $d = \frac{n_\phi(n_\phi+1)}{2}$, a lower bound on the number of samples N_s required to estimate Γ_v with confidence $1 - \beta$, is given as [36]:

$$N_s \geq \frac{2}{\delta} \left(\ln \frac{1}{\beta} + d \right). \quad (82)$$

For each $\theta_i = \text{vec}(A_i, B_i)$, we evaluate $\tilde{V}_i = \bar{V}_i - \hat{V}$ where the transfer matrix $\bar{V}_i = [\bar{V}_{i,1}, \dots, \bar{V}_{i,L}]$ is computed with A_i, B_i (cf. (18)). The bound Γ_v can be computed by solving the following SDP:

$$\begin{aligned} \min_{\Gamma_v} \quad & \text{trace}(\Gamma_v) \\ \text{s.t.} \quad & \Gamma_v \succeq \tilde{V}_i \tilde{V}_i^H, \quad i = 1, \dots, N_s. \end{aligned} \quad (83)$$

Scenario approach to estimate γ_y : Similar to Γ_v , the bound γ_y on the uncertain term $\|Y_{\text{tr}}\|$ in (35) is computed under the assumption that $\theta_{\text{tr}} \in \Theta_0$ in Appendix B. A tighter upper bound γ_y on $\|Y_{\text{tr}}\|$ can be computed by directly estimating an upper bound on $\|Y_{\text{tr}}\|$. To this end, given a probability of violation δ , we generate N_s samples of $\text{vec}(A_i, B_i) = \theta_i \in \Theta_0$, $i = 1, \dots, N_s$, from the multivariate normal distribution with mean $\hat{\theta}_{\text{prior}}$ and covariance $\Sigma_{\theta, \text{prior}}$ according to (82) with $d = 1$. For each A_i , we evaluate $\bar{Y}_i = [\bar{Y}_{i,1}, \dots, \bar{Y}_{i,L}]$ (cf. (18)). The bound γ_y can be computed as

$$\gamma_y = \max_{i=1, \dots, N_s} \|\bar{Y}_i\|. \quad (84)$$

The constants Γ_v and γ_y computed via the scenario approach ensure the same properties described in Sections IV-D, and hold jointly with confidence $1 - 2\beta$.

APPENDIX D SPECTRAL LINE OF PROCESS NOISE

By Parseval's theorem, we have

$$\sum_{k=0}^{T-1} w_k^\top w_k = \frac{1}{T} \sum_{i=0}^{T-1} \mathbf{w}(e^{j\omega_i})^\top \mathbf{w}(e^{j\omega_i}) \quad (85)$$

where $\omega_i = \frac{i}{T}$, $i = 0, \dots, T-1$. The amplitude of the spectral line of w_k is given by $\bar{w}(\omega_i) = \frac{\mathbf{w}(e^{j\omega_i})}{T}$ and hence,

$$\sum_{k=0}^{T-1} w_k^\top w_k = T \sum_{i=0}^{T-1} \bar{w}(\omega_i)^\top \bar{w}(\omega_i).$$

From this, we get $\sigma_w^2 I = T\sigma_{\bar{w}}^2 I$. Therefore, the radius $\sigma_{\bar{w}}$ of the spectral line of the process noise is

$$\sigma_{\bar{w}} = \frac{\sigma_w}{\sqrt{T}}. \quad (86)$$

APPENDIX E PROOF OF LEMMA 5

Proof. The proof follows the arguments in [35, Prop. 3.13, Sec. 4.2.5] and [25] for LPV control. First, note that the set definitions Δ_s, Δ_u can be equivalently represented as $\Delta_s \in \mathbf{\Delta}_s := \{\Delta : \lambda_s R_s - \lambda_s \Delta^\top \Delta \succ 0\}$ and $\Delta_u \in \mathbf{\Delta}_u := \{\Delta : \lambda_u R_u - \lambda_u \Delta^\top \Delta \succ 0\}$ with arbitrary positive scalars $\lambda_s, \lambda_u > 0$. Define $X = N^{-1}$ and $K_x = MN^{-1}$. Using the Schur complement for the inequality in (52a), and multiplying (52a) and (52b) by $\text{diag}(N^{-1}, I, I, I)$ and $\text{diag}(N^{-1}, I)$, respectively, from the left and the right yields

$$\begin{bmatrix} * \\ * \\ * \\ * \\ * \\ * \\ * \end{bmatrix}^\top \begin{bmatrix} -X & 0 & 0 & 0 & 0 & 0 \\ 0 & X & 0 & 0 & 0 & 0 \\ 0 & 0 & \lambda_s P_s & 0 & 0 & 0 \\ 0 & 0 & 0 & 0 & 0 & 0 \\ 0 & 0 & 0 & 0 & \lambda_u P_u & 0 \\ 0 & 0 & 0 & 0 & 0 & -\gamma_p I \\ 0 & 0 & 0 & 0 & 0 & -\gamma_p I \end{bmatrix} \times \begin{bmatrix} I & 0 & 0 & 0 \\ \hat{A}_0 + \hat{B}_0 K_x & I + \hat{B}_0 K_s & I & I \\ 0 & I & 0 & 0 \\ \begin{bmatrix} I \\ K_x \end{bmatrix} & \begin{bmatrix} 0 \\ K_s \end{bmatrix} & 0 & 0 \\ 0 & 0 & I & 0 \\ \begin{bmatrix} I \\ K_x \end{bmatrix} & \begin{bmatrix} 0 \\ K_s \end{bmatrix} & 0 & 0 \\ 0 & 0 & 0 & I \end{bmatrix} \prec 0, \quad (87a)$$

$$\begin{bmatrix} X & (C + DK_x)^\top \\ (C + DK_x) & Z \end{bmatrix} \succ 0, \quad (87b)$$

$$\text{trace}(Z) \leq \gamma_p, \quad (87c)$$

where $P_s = \begin{bmatrix} -I & 0 \\ 0 & R_s \end{bmatrix}$ and $P_u = \begin{bmatrix} -I & 0 \\ 0 & R_u \end{bmatrix}$. Using [25], [35], H_2 performance is guaranteed if there exists a positive definite matrix $X = X^\top \succ 0$ and Z satisfying the matrix inequalities (87). $X \succ 0$ follows from (87) with $N = X^{-1} \succ 0$. \square

REFERENCES

- [1] B. Recht, "A tour of reinforcement learning: The view from continuous control," *Annual Review of Control, Robotics, and Autonomous Systems*, vol. 2, pp. 253–279, 2019.
- [2] A. A. Feldbaum, "Dual control theory," *Automation and Remote Control*, vol. 21, no. 9, pp. 874–1039, 1960.
- [3] N. M. Filatov and H. Unbehauen, "Survey of adaptive dual control methods," *IEE Proceedings-Control Theory and Applications*, vol. 147, no. 1, pp. 118–128, 2000.
- [4] A. Mesbah, "Stochastic model predictive control with active uncertainty learning: a survey on dual control," *Annual Reviews in Control*, vol. 45, pp. 107–117, 2018.
- [5] E. Tse, Y. Bar-Shalom, and L. Meier, "Wide-sense adaptive dual control for nonlinear stochastic systems," *IEEE Transactions on Automatic Control*, vol. 18, no. 2, pp. 98–108, 1973.
- [6] E. Tse and Y. Bar-Shalom, "Actively adaptive control for nonlinear stochastic systems," *Proceedings of the IEEE*, vol. 64, no. 8, pp. 1172–1181, 1976.
- [7] D. S. Bayard and M. Eslami, "Implicit dual control for general stochastic systems," *Optimal Control Applications and Methods*, vol. 6, no. 3, pp. 265–279, 1985.

- [8] Y. Bar-Shalom and E. Tse, "Caution, probing, and the value of information in the control of uncertain systems," in *Annals of Economic and Social Measurement, Volume 5, number 3*, pp. 323–337, NBER, 1976.
- [9] B. Wittenmark, "Adaptive dual control methods: An overview," in *Adaptive Systems in Control and Signal Processing 1995*, pp. 67–72, Elsevier, 1995.
- [10] M. Gevers, "Identification for control: From the early achievements to the revival of experiment design," *European journal of control*, vol. 11, pp. 1–18, 2005.
- [11] H. Hjalmarsson, "From experiment design to closed-loop control," *Automatica*, vol. 41, no. 3, pp. 393–438, 2005.
- [12] M. Annergren, C. A. Larsson, H. Hjalmarsson, X. Bombois, and B. Wahlberg, "Application-oriented input design in system identification: Optimal input design for controls," *IEEE Control Systems Magazine*, vol. 37, no. 2, pp. 31–56, 2017.
- [13] C. A. Larsson, A. Ebadat, C. R. Rojas, X. Bombois, and H. Hjalmarsson, "An application-oriented approach to dual control with excitation for closed-loop identification," *European Journal of Control*, vol. 29, pp. 1–16, 2016.
- [14] T. A. N. Heirung, B. E. Ydstie, and B. Foss, "Dual adaptive model predictive control," *Automatica*, vol. 80, pp. 340–348, 2017.
- [15] M. Barentin and H. Hjalmarsson, "Identification and control: Joint input design and H_∞ state feedback with ellipsoidal parametric uncertainty via Imis," *Automatica*, vol. 44, no. 2, pp. 543–551, 2008.
- [16] X. Bombois, G. Scorletti, M. Gevers, P. M. Van den Hof, and R. Hildebrand, "Least costly identification experiment for control," *Automatica*, vol. 42, no. 10, pp. 1651–1662, 2006.
- [17] X. Bombois, F. Morelli, H. Hjalmarsson, L. Bako, and K. Colin, "Robust optimal identification experiment design for multisine excitation," *Automatica*, vol. 125, p. 109431, 2021.
- [18] J. Umenberger, M. Ferizbegovic, T. B. Schön, and H. Hjalmarsson, "Robust exploration in linear quadratic reinforcement learning," in *Advances in Neural Information Processing Systems*, pp. 15310–15320, 2019.
- [19] M. Ferizbegovic, J. Umenberger, H. Hjalmarsson, and T. B. Schön, "Learning robust LQ-controllers using application oriented exploration," *IEEE Control Systems Letters*, vol. 4, no. 1, pp. 19–24, 2019.
- [20] A. Iannelli, M. Khosravi, and R. S. Smith, "Structured exploration in the finite horizon linear quadratic dual control problem," in *Proc. 21st IFAC World Congress*, pp. 959–964, 2020.
- [21] J. Venkatasubramanian, J. Köhler, J. Berberich, and F. Allgöwer, "Robust dual control based on gain scheduling," in *Proc. 59th IEEE Conference on Decision and Control (CDC)*, pp. 2270–2277, IEEE, 2020.
- [22] C. R. Rojas, J. S. Welsh, G. C. Goodwin, and A. Feuer, "Robust optimal experiment design for system identification," *Automatica*, vol. 43, no. 6, pp. 993–1008, 2007.
- [23] A. Sarker, P. Fisher, J. E. Gaudio, and A. M. Annaswamy, "Accurate parameter estimation for safety-critical systems with unmodeled dynamics," *Artificial Intelligence*, vol. 316, p. 103857, 2023.
- [24] P. Rigollet and J.-C. Hütter, "High dimensional statistics," *Lecture notes for course 18S997*, vol. 813, p. 814, 2015.
- [25] C. W. Scherer, "LPV control and full block multipliers," *Automatica*, vol. 37, no. 3, pp. 361–375, 2001.
- [26] J. Veenman and C. W. Scherer, "A synthesis framework for robust gain-scheduling controllers," *Automatica*, vol. 50, no. 11, pp. 2799–2812, 2014.
- [27] F. Paganini and E. Feron, "Linear matrix inequality methods for robust h2 analysis: A survey with comparisons," in *Advances in linear matrix inequality methods in control*, pp. 129–151, SIAM, 2000.
- [28] A. Sarker, P. Fisher, J. E. Gaudio, and A. M. Annaswamy, "Corrigendum to "accurate parameter estimation for safety-critical systems with unmodeled dynamics" [artif. intell. 316 (2023) 103857]," *Artif. Intell.*, vol. 317, apr 2023.
- [29] R. J. Caverly and J. R. Forbes, "Lmi properties and applications in systems, stability, and control theory," *arXiv preprint arXiv:1903.08599*, 2019.
- [30] S. P. Boyd and L. Vandenberghe, *Convex optimization*. Cambridge university press, 2004.
- [31] L. Pronzato, "Optimal experimental design and some related control problems," *Automatica*, vol. 44, no. 2, pp. 303–325, 2008.
- [32] S. Dean, H. Mania, N. Matni, B. Recht, and S. Tu, "On the sample complexity of the linear quadratic regulator," *Foundations of Computational Mathematics*, pp. 1–47, 2019.
- [33] M. Grant and S. Boyd, "CVX: MATLAB software for disciplined convex programming, version 2.1," Mar. 2014.
- [34] A. Tsiamis and G. J. Pappas, "Linear systems can be hard to learn," in *Proc. 2021 60th IEEE Conference on Decision and Control (CDC)*, pp. 2903–2910, IEEE, 2021.
- [35] C. Scherer and S. Weiland, "Linear matrix inequalities in control," *Lecture Notes, Dutch Institute for Systems and Control, Delft, The Netherlands*, vol. 3, 2000.
- [36] M. C. Campi, S. Garatti, and M. Prandini, "The scenario approach for systems and control design," *Annual Reviews in Control*, vol. 33, no. 2, pp. 149–157, 2009.



Janani Venkatasubramanian received her Master degree in Electrical Engineering from the Delft University of Technology, The Netherlands, in 2018. Since May 2019, she is a Ph.D. student at the Institute for Systems Theory and Automatic Control, University of Stuttgart under the supervision of Prof. Frank Allgöwer, and a member of the International Max Planck Research School for Intelligent Systems (IMPRS-IS). Her research interests lie in the area of learning and adaptive control.



Johannes Köhler received his Master degree in Engineering Cybernetics from the University of Stuttgart, Germany, in 2017. In 2021, he obtained a Ph.D. in mechanical engineering, also from the University of Stuttgart, Germany, for which he received the 2021 European Systems & Control Ph.D. award. He is currently a postdoctoral researcher at the Institute for Dynamic Systems and Control (IDSC) at ETH Zürich. His research interests are in the area of model predictive control and control and estimation for nonlinear uncertain systems.



Julian Berberich received a Master's degree in Engineering Cybernetics from the University of Stuttgart, Germany, in 2018. In 2022, he obtained a Ph.D. in Mechanical Engineering, also from the University of Stuttgart, Germany. He is currently working as a Lecturer (Akademischer Rat) at the Institute for Systems Theory and Automatic Control at the University of Stuttgart, Germany. In 2022, he was a visiting researcher at the ETH Zürich, Switzerland. He has received the Outstanding Student Paper Award at the 59th IEEE Conference on Decision and

Control in 2020 and the 2022 George S. Axelby Outstanding Paper Award. His research interests include data-driven analysis and control as well as quantum computing.



Frank Allgöwer is professor of mechanical engineering at the University of Stuttgart, Germany, and Director of the Institute for Systems Theory and Automatic Control (IST) there. Frank is active in serving the community in several roles: Among others he has been President of the International Federation of Automatic Control (IFAC) for the years 2017-2020, Vice-president for Technical Activities of the IEEE Control Systems Society for 2013/14, and Editor of the journal *Automatica* from 2001 until 2015. From 2012 until 2020 Frank served in

addition as Vice-president for the German Research Foundation (DFG), which is Germany's most important research funding organization. His research interests include predictive control, data-based control, networked control, cooperative control, and nonlinear control with application to a wide range of fields including systems biology.